Chemical Science

Accepted Manuscript

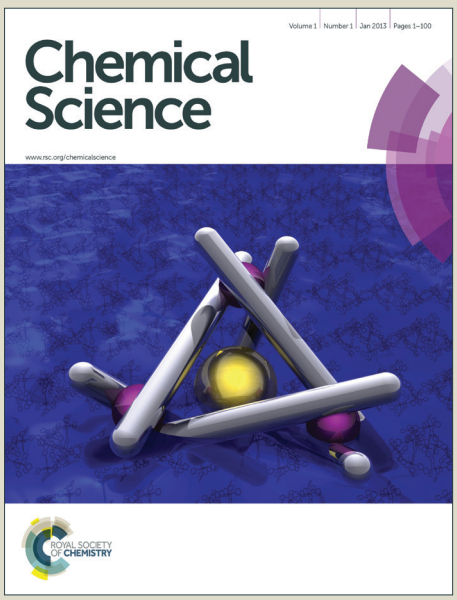

This is an *Accepted Manuscript*, which has been through the Royal Society of Chemistry peer review process and has been accepted for publication.

Accepted Manuscripts are published online shortly after acceptance, before technical editing, formatting and proof reading. Using this free service, authors can make their results available to the community, in citable form, before we publish the edited article. We will replace this *Accepted Manuscript* with the edited and formatted *Advance Article* as soon as it is available.

You can find more information about *Accepted Manuscripts* in the Information for Authors.

Please note that technical editing may introduce minor changes to the text and/or graphics, which may alter content. The journal's standard Terms & Conditions and the Ethical guidelines still apply. In no event shall the Royal Society of Chemistry be held responsible for any errors or omissions in this *Accepted Manuscript* or any consequences arising from the use of any information it contains.

ROYAL SOCIETY OF CHEMISTRY

www.rsc.org/chemicalscience

Joining Forces: Integrating the Mechanical and Optical Single Molecule Toolkits

Monique J. Jacobs and Kerstin Blank*

Radboud University Nijmegen, Institute for Molecules and Materials, Department of Molecular Materials, Heyendaalseweg 135, 6525 AJ Nijmegen, The Netherlands

*corresponding author:

email: k.blank@science.ru.nl

phone: +31-24-365 24 64

fax: +31-24-365 29 29

Chemical Science Accepted Manuscript

Abstract

Single molecule force spectroscopy and single molecule fluorescence microscopy have both evolved into extremely powerful tools for studying molecular mechanisms in Biophysics and Materials Science. Recent technological developments have focused on combining the strengths of both techniques in one instrument. Integrated instruments provide unique possibilities for mechanically manipulating a single molecule while observing its response optically. Here we provide an overview of the state-of-the-art with an emphasis on the technological challenges. Describing the mostly biological systems that have been studied to date, we discuss the application of combined force-fluorescence approaches for studying force-structure-function relationships. We further highlight the potential of integrated setups for investigating mechanosensing and mechanoregulation in biological systems and for characterizing molecular force probes that find potential application in (biomimetic) self-reporting and self-healing materials.

Keywords

single molecule fluorescence, force spectroscopy, optical tweezers, magnetic tweezers, AFM, confocal, TIRF, force sensor, mechanosensing, mechanoregulation, mechanophore, mechanochemistry, DNA, protein

Chemical Science Accepted Manuscript

Table of Contents Entry

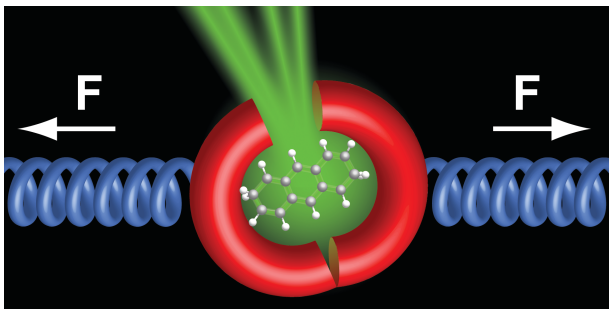

Combining single molecule force measurements with fluorescence detection opens up exciting new possibilities for the characterization of mechanoresponsive molecules in Biology and Materials Science.

Chemical Science Accepted Manuscript

Introduction

Understanding mechanical processes at the molecular level is a crucial aspect of both Materials Science and Biology. Biological systems utilize mechanical information to sense and interact with their environment. Mechanical signals are, for example, involved in cancer metastasis[1] and stem cell differentiation[2] where they appear to be equally important as biochemical signals. The mechanical properties of many cells and tissues have been investigated[3–5] and the downstream cellular response following a mechanical stimulation has been recorded for a number of systems.[6] Although several key players have been identified, still little is known about the proteins that sense the mechanical signal and convert it into the biochemical response, *i.e.* the molecular force sensors. In general, force acting on a protein is believed to trigger a conformational change. This conformational change might in turn lead to the exposure of cryptic sites that facilitate ligand binding (*e.g.* talin[7] and fibronectin[8]), become accessible for protease cleavage (*e.g.* collagen,[9] the Notch receptor[10] and van Willebrand factor[11]) or become enzymatically active themselves (*e.g.* titin kinase[12,13]). Alternatively, the applied force might strengthen a receptor ligand interaction (*e.g.* the catch bonds observed for selectins[14] and the bacterial adhesin FimH[15]) ensuring that it withstands the mechanical stress.

From a Materials Science perspective mechanoresponsive biological systems are highly sophisticated functional materials that have evolved impressive self-reporting and self-healing properties.[16] Biological systems are consequently an important source of inspiration for designing novel materials with these properties. But also purely synthetic mechanoresponsive molecules (mechanophores) have been developed in recent years. Mechanochemistry, *i.e.* the design, synthesis and characterization of synthetic mechanophores, is a rapidly growing field of research.[17–19] Many interesting molecular designs have been implemented such as predetermined mechanical breaking points,[19–21] mechanochromic dyes[22,23] and mechanically activated latent catalysts.[24–26]

Chemical Science Accepted Manuscript

A detailed understanding of force-structure-function relationships is essential for establishing the mechanisms of biological force sensing and for the systematic design of synthetic mechanophores. A crucial bottleneck is the lack of characterization methods that allow for quantifying the molecular forces while at the same time correlating the mechanical stimulus with the observed change in function. Synthetic mechanophores are mostly characterized using ensemble techniques[27] such as tensile testing instruments[23] or ultrasound polymer mechanochemistry[19,21,24–26] whereas biological force sensors are frequently characterized using single molecule force spectroscopy. The single molecule force spectroscopy toolkit allows for the direct application of a defined force to a single molecule. The applied force is a well-controlled external parameter that leads to a defined and quantifiable change in the energy landscape of the molecule or molecular interaction.[28,29] Measuring stabilities and kinetics at different forces further allows extrapolation to "force-free" conditions using well-established theoretical models.[30–32] Considering the versatility of this approach, single molecule methods have great potential for the characterization of synthetic mechanophores where little information about the molecular forces is currently available.

Single molecule force spectroscopy is powerful, but cannot always report on the mechanically induced change in structure or function. This is only possible when the mechanical manipulation leads to bond rupture[9,14,15] or when it alters the length of the molecule.[22,33] Not all mechanoresponsive molecules, however, react to the mechanical stimulus in a way that allows a force spectroscopy-based readout. Single molecule fluorescence microscopy provides a complementary strategy. Combining the two approaches adds many new possibilities for detecting a force-induced molecular response such as a conformational change, a binding event or a catalytic reaction. Consequently, the high interest in mechanosensing in biological and synthetic systems has motivated many recent efforts to combine force spectroscopy with single molecule fluorescence detection.

Chemical Science Accepted Manuscript

In this Perspective we aim to introduce the reader to the currently used approaches for combining single molecule force spectroscopy with fluorescence measurements. After briefly describing the commonly used force and fluorescence techniques, we will discuss specific challenges arising from combining these techniques. We will describe the strategies developed to overcome these obstacles and introduce the molecular systems that have been characterized using combined approaches. Not all of them are necessarily directly involved in mechanosensing. We rather aim to provide a comprehensive overview of the many different possibilities of establishing force-structure-function relationships. We believe that the instrumental setups and experimental strategies developed can be applied broadly and will be of crucial importance for the future characterization of mechanically responsive molecules. Mechanical insight can also be obtained using a number of alternative techniques such as flow-stretching assays or rheology even though they do not always allow for a direct quantification of the force at the single molecule level. After a short summary of these techniques, we will conclude this Perspective with a short overview of the current designs of biological molecular force sensors and synthetic mechanophores. These molecular force probes can potentially replace macroscopic force probes and allow for *in situ* force measurements in biological systems and self-reporting materials.

Single Molecule Force Spectroscopy (SMFS)

Mechanical single molecule manipulation and detection requires a force probe that is directly attached to the target molecule allowing for the application of the force. Using optical tweezers (OTs), magnetic tweezers (MTs) and the atomic force microscope (AFM), this force can be directly quantified after calibration of the force probe. The application of these techniques is mostly determined by their specific range of operation characterized by the linear force range and the stiffness of the force probe (Figure 1). The stiffness of the force probe describes its

Chemical Science Accepted Manuscript

resistance to deformation and, consequently, determines how fast it reacts to movements of the attached molecule. When using a low-stiffness force probe, small deviations in the location of the molecule have only a minor effect on the force applied. This is a clear advantage for applications where the force acting on the molecule needs to be held constant (force-clamp), especially in the low force range. On the other hand, a low stiffness limits the applicability of the force probe for applications where the force acting on the molecule needs to be increased (force-ramp). A stiff force probe allows for faster adjustments of the force in these applications. Obviously, stiff probes in force-clamp applications react to minor displacements of the attached molecule causing a high noise level. When describing the different techniques in the following, we are focusing on the aspects most relevant for combining these techniques with single molecule fluorescence microscopy. Several excellent reviews describing force-based single molecule techniques in more detail have been published recently.[34–38]

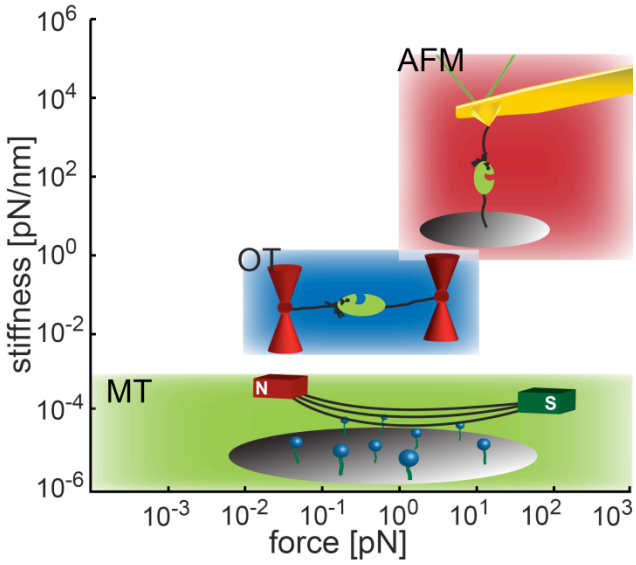

Figure 1. Comparison of the three most common force spectroscopy techniques. While the force range partly overlaps, the stiffness is unique for the three different instruments. Atomic force microscopy (AFM) and optical tweezers (OT) are usually limited to one molecule under force at a time. In contrast, magnetic tweezers (MT) allow for multiplexing.

Chemical Science Accepted Manuscript

Atomic force microscopy

The atomic force microscope (AFM) is widely known for its imaging capability, allowing for the depiction of biological samples under ambient conditions with sub-nanometer resolution.[39] Apart from imaging, which lies beyond the scope of this review, the AFM is a versatile single molecule force tool. Its principle of operation is based on the law of levers. A sharp tip is attached to a flexible cantilever and the molecule of interest is immobilized between the tip and a surface. Movements of the tip, resulting from a response of the molecule, are detected using a laser that is focused on the back of the cantilever and reflected onto a photosensitive diode. In this way, very small vertical and horizontal movements of the tip can be recorded and forces between 10 pN and 100 nN are detected. The AFM covers a big force range and reaches a time resolution down to the sub-millisecond range. It allows for both force-ramp and for force-clamp applications although OTs and MTs are superior for force-clamp measurements in the low force range.

Optical tweezers

Since their invention by Arthur Ashkin in 1986,[40] optical tweezers (OTs) have rapidly become a standard tool in single molecule manipulation. They utilize optical gradient forces: when a laser beam is focused, a strong electrical field gradient is generated in the beam waist, which attracts dielectric microparticles towards the waist center. Force readout is achieved by monitoring the light scattered by the trapped particle using a quadrant-photodiode. The force generated by the field gradient is usually in the pN range and linearly decreases for short displacements off the center.

In most biological applications polystyrene beads are used for trapping as the biomolecule of interest can be coupled to the bead easily. To apply a force on the molecule, a second attachment point is needed which can either be the surface of the sample chamber, a second bead held by a micropipette or a second bead in another optical trap. To uncouple the target

Chemical Science Accepted Manuscript

molecule completely from external vibrations, a configuration with two optical traps is the method of choice (Dumbbell configuration[41]). This method is technically more challenging but allows for 3D manipulation with low noise and low drift. Depending on the geometry of the setup, optical tweezers cover a force range of 0.1 pN up to 100 pN, have a temporal resolution between 0.2 ms to 20 ms and can achieve sub-nanometer spatial resolution. OTs are used for both force-ramp and force-clamp experiments.

Magnetic tweezers

Magnetic tweezers (MTs) consist of a pair of magnets (permanent or electromagnetic) on top of a sample chamber. Paramagnetic beads, immersed in the sample chamber, are attracted to the magnets. This allows for stretching molecules that are coupled to both the beads and the bottom surface of the sample chamber. Brownian motion of the beads varies as a function of the applied force and can be used as an indirect readout. Bead motion is detected optically with a time resolution between 1 ms and 100 ms. Movement in the x- and y-direction is determined by tracking the center of the bead's interference fringes. Variation in the fringe pattern gives information on the relative z-position with an accuracy down to 10 nm. Magnetic tweezers can cover a huge force range from 10^{-3} pN to 10^{4} pN.

One key characteristic of MTs is their low stiffness making force fluctuations negligible even in the low force range. At the same time it is difficult to increase the force quickly and the beads would have to be moved over long distances to alter the force. The magnetic field can only be modified slowly, however, and the big magnetic beads cause hydrodynamic drag. MTs are consequently hardly used in force-ramp experiments, but are ideal for force-clamp experiments. MTs allow for measuring many molecules in parallel. The magnets generate a magnetic field gradient that is orders of magnitude bigger than the size of the magnetic beads, so that the same force can be applied to several beads simultaneously, increasing the throughput. Lastly, MTs can be used to simultaneously apply torque to a molecule by rotating the magnetic field,[42]

Chemical Science Accepted Manuscript

a feature that cannot be achieved with AFM and requires advanced setups with optical tweezers.[43]

Single Molecule Fluorescence Microscopy (SMFM)

Single molecule fluorescence microscopy aims to optically detect the location of target molecules by specifically labeling them with fluorophores. The spatial resolution is normally diffraction limited to ~200 nm. But smaller objects down to 2 - 20 nm can be localized or resolved by using techniques such as FIONA (fluorescence imaging with one nanometer accuracy),[44] STED (stimulated emission depletion),[45] SOFI (super-resolution optical fluctuation imaging)[46] or any of the superresolution imaging techniques based on stochastic localization.[47–49] In addition, time-dependent processes can be followed. SMFM offers a wide range of time scales, from microseconds to seconds, depending on the detector hardware and the area imaged (widefield *vs.* confocal detection). Single molecule fluorescence is consequently not only used to image but also to track the movement of fluorescently labeled molecules and to follow dynamic processes within one molecule such as catalytic events[50,51] or conformational changes.[52–54] Conformational changes occur on the 0.1 nm – 10 nm length scale and require FRET-based[55] (Fluorescence Resonance Energy Transfer; distance fluctuations between 2 – 8 nm), or electron transfer-based[56] (below 1 nm) reporter systems. Fluorescence-based optical approaches for studying single molecules are commonly used and we will only briefly summarize their main characteristics. The interested reader is referred to more detailed reviews on single molecule fluorescence.[57–59]

Widefield fluorescence microscopy

In widefield epifluorescence microscopy the desired area of the sample is illuminated and imaged with a field of view of up to 2 x 2 mm^2 depending on the magnification used. CCD

Chemical Science Accepted Manuscript

cameras are the most frequently used detectors. The optical geometry is simple and features anywhere within the sample can be monitored. Most importantly, camera detection allows for monitoring many molecules in parallel, providing statistics from a large number of individual molecules. As a result of the camera detection, the temporal resolution is limited to the millisecond range. Besides the low temporal resolution, epifluorescence microscopy suffers from a low signal-to-noise (S:N) ratio. A crucial factor limiting the S:N ratio of the instrument is the detection volume. While the signal scales linearly, the background intensity scales to the power of three with the detection volume. Widefield TIRF (Total Internal Refection Fluorescence) microscopy restricts the detection volume to a thin layer (~200 nm) illuminated by a standing wave (evanescent field) near a dielectric interface. This surface can either be a prism or a cover slip in objective-based TIRF. In this way, TIRF achieves high S:N ratios while providing the possibility of observing many molecules in parallel.

Confocal fluorescence microscopy

In a confocal microscope the detection is limited to one point on the sample using a diffraction limited laser spot to excite the fluorophores. The detection volume is further restricted in the z-direction by placing a small (50 - 100 µm) pinhole in the detection path. In this way, only in-focus light originating from a small (0.5 - 1 femtoliter) spheroidal volume within the sample is allowed to reach the detector. For single molecule detection, avalanche photodiodes provide the required sensitivity and a superior time resolution in the nanosecond range. To obtain an image in order to find a target molecule, the surface needs to be scanned in a raster like fashion, also restricting the statistics to one molecule at a time. In contrast to widefield TIRF microscopy, confocal detection is not limited to molecules close to a surface.

Chemical Science Accepted Manuscript

Combined Single Molecule Force - Fluorescence Approaches

As powerful as force spectroscopy and fluorescence microscopy are individually, their combination allows for addressing unique questions that cannot be answered with any single technique alone. To take maximum advantage of a combined force-fluorescence instrument, the two techniques should complement their strengths. Ideally they should match in temporal as well as spatial resolution and have the same ability for multiplexing.

Most importantly, the combined use of both techniques should not hamper either technique's performance. Each technique has its own specific requirements and the interplay of the two might come at the price of combination-specific drawbacks: the presence of a force probe might increase the fluorescence background and the presence of an optical detection pathway might add vibrations that couple into the force detection system. In general, experiments that require a simultaneous measurement of both force and fluorescence are far more challenging to implement. Sequential operation of both detection principles is the easiest strategy to avoid interference between them. On the other hand, the full potential of a combined setup can only be exploited when one technique is used for manipulation, while the other provides simultaneous readout.

Combining AFM-force spectroscopy with fluorescence

Combined AFM-fluorescence setups have originally been developed for imaging applications and are commonly used to overlay AFM topography images with fluorescence data. Instruments for sequential AFM and fluorescence imaging are commercially available[60] and the applications have been reviewed elsewhere.[6] More recently, combined AFM-fluorescence instruments have been used for applying and measuring forces. Before a combined AFM-fluorescence setup can be used for a simultaneous measurement of force and fluorescence, the following problems need to be overcome: the AFM laser as well as the AFM tip might interfere with the

Chemical Science Accepted Manuscript

fluorescence signal. Further, vibrations from the optics setup can couple into the sample affecting the force-resolution of the AFM.[61]

Addressing the problem of the AFM laser interfering with the optical signal, AFM manufacturers have reacted to the increasing demand of AFMs compatible with fluorescence microscopes. They offer AFM-lasers in the IR range equipped with additional filters to lower the interference with commonly used dyes in the visible spectral range.[60] Depending on their material and shape, AFM cantilevers show autofluorescence or affect the fluorescence signal otherwise. A systematic study performed by Gaiduk *et al.*[62] showed that the relative fluorescence intensity of the AFM-cantilever further depends on the distance of the tip apex from the imaging plane. At >300 nm separation, the signal for silicon nitride (Si_3N_4) cantilevers is below the single molecule detection limit and does no longer interfere with fluorescence measurements. The short penetration depth of the evanescent field of objective-based TIRF microscopes (~200 nm) thus reduces the problem of tip autofluorescence or scattering in most cases. 'Biolever mini' cantilevers, made of pure silicon, display intrinsically low autofluorescence.[63] They seem to be the perfect choice for combined single molecule fluorescence and force spectroscopy as they also fulfill the need for small cantilevers for force spectroscopy.[64] Unfortunately, it is difficult to focus especially the long wavelength AFM lasers on the back of these cantilevers. Stray light may be reflected from the sample surface and cause optical interferences with the actual AFM signal, dramatically compromising the resolution.

The major issue that limits the performance of the AFM in combined instruments are vibrations that couple into the sample.[61] The instrument can be protected easily from typical noise sources such as acoustic noise and vibrations of the building by placing it into a soundproof box and onto an active table. Noise sources from inside the instrument remain problematic, however. Due to geometrical considerations, prism-based TIRF cannot be combined with AFM, so that objective-based TIRF or confocal setups need to be used. The required objectives have very short working distances and require thin cover slips (<0.2 mm) to mount the sample. These thin

Chemical Science Accepted Manuscript

cover slips are susceptible to vibrations. Gumpp *et al.*[61] compared the height fluctuations of the cover slip surface for a standard commercial TIRF microscope with an objective revolver, a setup with a piezo moving the objective for focusing and a setup with a fixed objective and a moveable tube lens.[61] Both setups that had the focusing mechanism connected to the objective suffered from cover slip vibrations of ±1 nm. Only the setup with the fixed objective showed significantly reduced vibrations permitting high-resolution single molecule force spectroscopy (Figure 2).

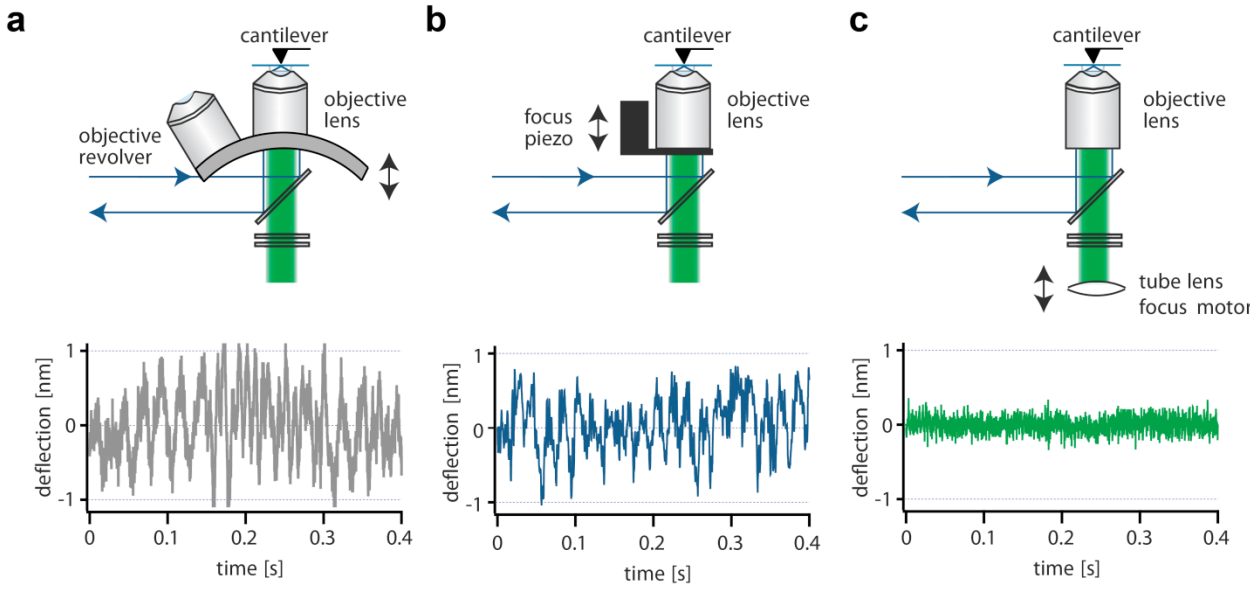

Figure 2. Height fluctuations of the cover slip surface determined for different AFM-TIRF microscope designs with (a) an objective revolver (standard configuration), (b) a piezo for focusing the objective lens and (c) a setup with fixed objective and movable tube lens for focusing. Reprinted with permission from Gumpp *et al*. Rev. Sci. Instrum., 2009, 80, 063704.[61] Copyright 2009 AIP Publishing LCC.

As a direct consequence of the above problems, only a small number of experiments have been performed to date where force and fluorescence detection were performed simultaneously. In most experiments the AFM tip was used to transport the molecule of interest to a specific area and the fluorescence was measured in subsequent steps. The high lateral resolution of the AFM

Chemical Science Accepted Manuscript

allows for the positioning of single molecules on a surface with nanometer accuracy. Making clever use of the shear and unzip geometry of DNA, Gaub and coworkers developed a cut-and-paste strategy that allowed for picking up individual DNA molecules from one area on a surface and delivering them onto another area (Figure 3).[65–69] Using a combined AFM-TIRF setup, the cut-and-paste process was followed by AFM and the assembled patterns as well as single deposited Cy3-dyes[68] were detected using the TIRF microscope.

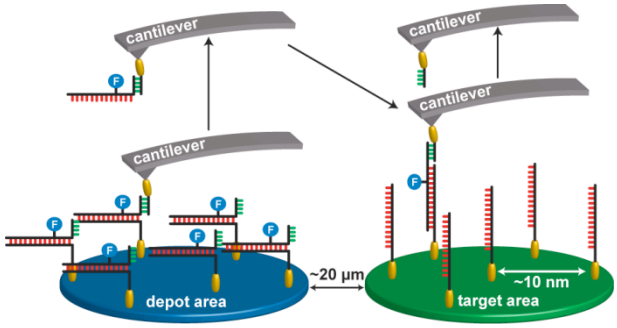

Figure 3. Single molecule cut-and-paste. The cut-and-paste process makes use of the hierarchical binding forces of 3 different DNA duplexes: $F_{unzip}<F_{shear1}<F_{shear2}$. A short strand of single stranded DNA (ssDNA) is coupled to the cantilever and hybridizes to complementary ssDNA in the depot area to yield a short duplex in shear configuration. This complementary sequence is connected to a double stranded DNA (dsDNA) duplex in unzipping configuration. As F_{unzip} is lower than F_{shear1}, the DNA is picked up by the AFM cantilever and can be delivered to the target area. On the target area, the ssDNA forms a duplex with a new DNA strand (F_{shear2}). Now two duplexes in shear configuration are stretched in series and compared with each other. The shorter duplex (F_{shear1}) ruptures, leaving the cantilever with the initial ssDNA. The cut-and-paste process is followed optically as the transferred DNA molecule is fluorescently labeled. Reprinted with permission from Cordes *et al.*, Nano Lett., 2010, 10, 645–651.[65] Copyright 2010 American Chemical Society.

Early experiments that combined mechanical manipulation of single molecules with simultaneous fluorescence readout mostly used biomolecules that were labeled with multiple

Chemical Science Accepted Manuscript

fluorophores. Several studies have been performed that attempted to relate the fluorescence signal of fluorescently labeled DNA[70,71] or titin[72] to an applied force. More recently, experiments with single fluorophore sensitivity have been set up to investigate the effect of force on enzymatic activity. Using a combined AFM-TIRF microscope, *Candida antarctica* lipase B (CalB) enzymes were stretched up to a threshold force defined by an antibody-antigen interaction (Figure 4). Meanwhile the enzymatic activity was followed by recording the cleavage of a fluorogenic substrate and a correlation between the force and activity cycles was observed.[73] More recently, the approach has been developed further for investigating the mechanical activation of the cryptic catalytic site in titin kinase.[13] The protein was positioned in a zero mode waveguide structure to reduce the detection volume. This allowed for the use of the fluorescently labeled substrate Cy3-ATP and substrate binding was detected for the stretched enzyme.

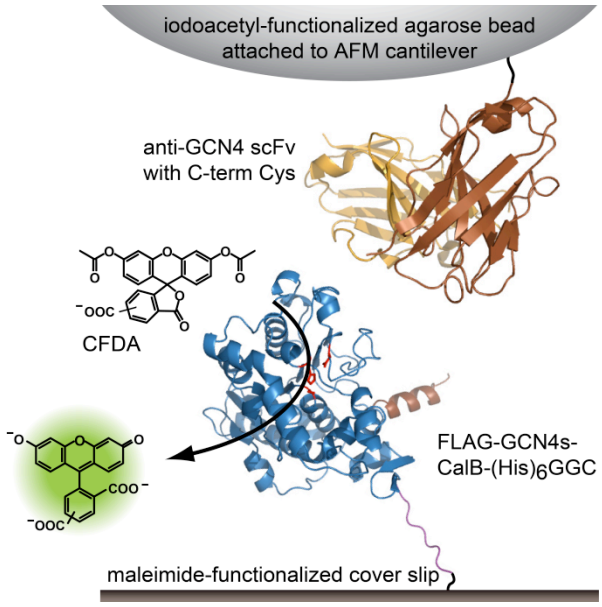

Figure 4. Experimental setup for the mechanical manipulation of the enzyme CalB with an AFM. To eliminate possible fluorescence background from the AFM cantilever an agarose bead was attached to the cantilever. The use of an antibody-antigen interaction (brown) facilitates reversible stretching and relaxation cycles of the enzyme (blue). The fluorogenic substrate 5,6-

Chemical Science Accepted Manuscript

carboxyfluorescein diacetate (CFDA) was used to detect enzymatic turnovers with a TIRF microscope.[73]

A combined AFM-confocal instrument was used to investigate domain unfolding of single HPPK (6-hydoxymethyl-7,8-dihydropterin pyrophosphokinase) enzymes. HPPK molecules were stretched while unfolding was monitored simultaneously using a single FRET pair.[74] Using the light scattered by the AFM tip, it was possible to align both the tip and the confocal volume at the position of a single enzyme. Both donor and acceptor fluorescence were detectable on top of the background signal originating from the tip and changes in the FRET efficiency could be measured during the approach and retract cycles.

In summary, the AFM is a powerful tool that can be combined with both confocal and TIRF microscopes. Overcoming the fluorescent background introduced by the AFM and the force vibrations originating from the optical detection system have been serious problems that are currently being solved. First real single molecule experiments are now possible and the potential of the combined approach can now be fully exploited.

Combining optical tweezers with fluorescence

Being a purely optical approach, the combination of OTs with single molecule fluorescence seems obvious. The same objective can be used for both, bead and fluorescence detection, using a dichroic mirror that separates the signals. Nevertheless, such a combination does not come without problems. Most fluorescent dyes show enhanced photobleaching when exposed to the high-intensity, near infrared trapping laser. The mechanism involves the absorption of two photons but is not yet fully understood. It might depend on the fluorophore used with, for example, Cy3 being far more sensitive than tetramethylrhodamine.[75,76] The biggest challenge in any combined OT-fluorescence setup is consequently the prevention of photobleaching of the fluorophore(s) to be detected. A number of different solutions have been implemented such as

Chemical Science Accepted Manuscript

labeling the molecule of interest with many fluorophores or using photostable quantum dots instead. Alternatively, the trapping laser can be spatially or temporarily separated from the part of the sample that contains the fluorescently labeled molecules to be studied. Depending on the fluorescence detection scheme used, single trap or dual trap configurations introduce additional challenges. Dual traps, for example, are difficult to combine with TIRF excitation. Due to the size of the beads used for trapping, the stretched molecule would be located outside the evanescent field. Single traps where the molecule is attached to the cover slip surface are an easy solution (Figure 5a). Alternatively, microfabricated glass pedestals can be used (Figure 5b). They can be placed between the trapped beads while serving as a prism for TIRF excitation.

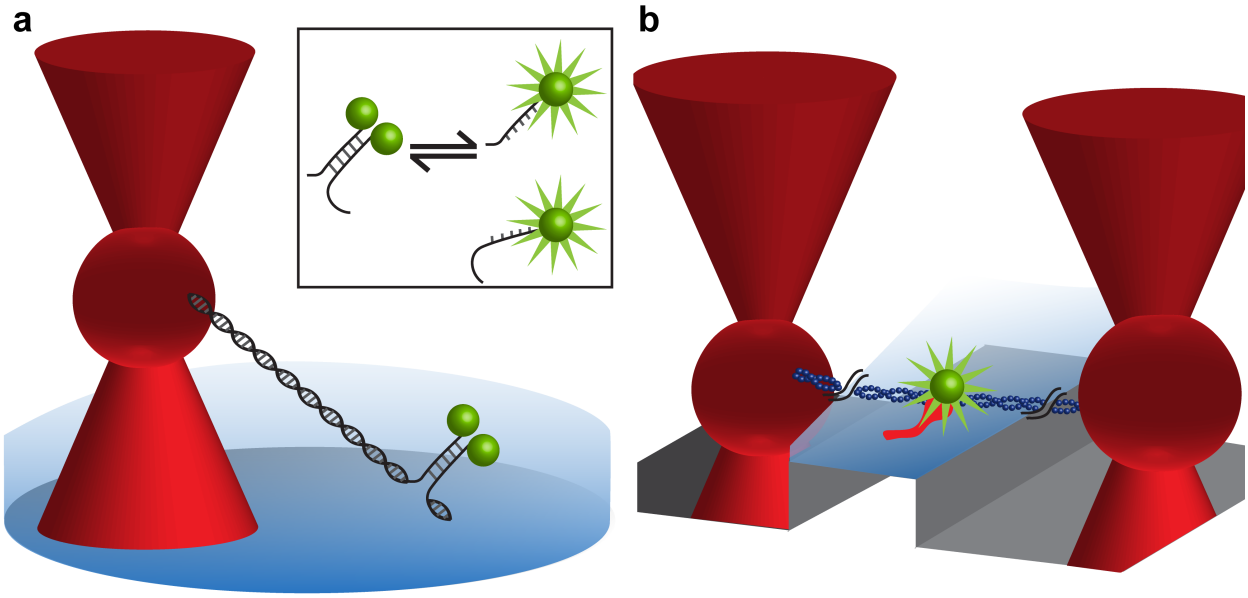

Figure 5. Experimental setups allowing for the combination of optical trapping with TIRF excitation. (a) single trap configuration as described by Lang *et al.*[77], showing the unzipping of dsDNA labeled with internally quenched fluorophores; (b) double trap configuration with a glass pedestal. This example illustrates actin being stretched between the traps. Myosin is immobilized on the glass pedestal, as described by Ishijima *et al.*[78]

The first experiment that combined optical tweezers with fluorescence detection was performed by Chu and coworkers in 1991.[79] The experiment was designed to study the elasticity of

Chemical Science Accepted Manuscript

fluorescently labeled DNA using a configuration with two optical traps and an image intensified video camera for fluorescence detection. In this experiment, enhanced photobleaching was a minor problem. The experiment was performed with a large DNA molecule (λ-DNA) that was stained with a very high number of ethidium bromide fluorophores. Using this strategy, it was possible for the first time to observe and manipulate a single DNA molecule. In a similar experiment, YOYO-1 labeled λ-DNA was stretched between an optical trap and a micropipette.[80] It was observed that YOYO-1 binding elongated the DNA by a factor of 1.2. At the same time, the orientation of the YOYO-1 dyes relative to the DNA axis was determined using fluorescence polarization.

While the above experiments aimed at the analysis of a single DNA molecule, they did not allow for observing single fluorophores. In one early experiment by Lang and coworkers[77] simultaneous single molecule force and fluorescence detection was performed using the above mentioned tetramethylrhodamine that is hardly affected by the trapping laser. In this experiment, the mechanical unzipping of a short DNA strand labeled with one fluorophore each was studied using a single trap configuration combined with TIRF excitation (Figure 5a). Initially quenched, the fluorescence was recovered when separating the DNA strands. In such a force-ramp experiment, the exposure of the fluorophores to the trapping laser and the excitation laser can be limited to the duration of the force-ramp preventing fast fluorophore inactivation.

In force-clamp experiments the fluorophore is usually exposed to the excitation and the trapping laser for significantly longer times. The use of quantum dots (QDs) as fluorescent labels provides a more general solution to the enhanced photobleaching problem due to their exceptional brightness and photostabiltiy. QDs have, for example, been used for labeling EcoRV enzymes. Sliding along a stretched DNA molecule, the diffusion constant of these QD-labeled enzymes was measured at the single molecule level using a setup combining two optical traps with brightfield fluorescence imaging.[81] In a similar experimental setup, using epifluorescence illumination, the feasibility of fluorescence imaging with nanometer accuracy

Chemical Science Accepted Manuscript

(FIONA) was investigated.[82] In this proof-of-principle experiment, a single QD was attached to an actin filament in the trap. The high brightness of the QD allowed its localization with an accuracy of 2 nm, which was similar to a QD immobilized on a glass surface. Although quantum dots as fluorescent labels offer a technically simple solution, their application introduces new challenges. Currently, their blinking behavior, their huge size as well as the lack of suitable coupling strategies restricts their applicability.[83]

Other experimental designs have been implemented to circumvent the problem of enhanced photobleaching while allowing for true single molecule fluorescence detection. A promising and straightforward strategy is the usage of long spacers to spatially separate the optical trap(s) from the fluorescence excitation area (Figure 5b and Figure 6). Using this approach, Yanagida and coworkers were the first to observe single myosin molecules while walking on a stretched actin filament.[84] After binding of the fluorescently labeled myosin molecule to the actin filament held between two optical traps, its movement along the 15 μm long filament was followed in an epifluorescence microscope. Using a modified experimental setup, single ATP turnovers were observed that correlated with myosin walking.[78] Following these initial experiments, TIRF excitation with microfabricated glass pedestals (Figure 5b) was subsequently implemented to improve the S:N ratio.[78] Cy5-labeled myosin molecules were immobilized on the glass pedestal and a Cy5-labeled actin filament was stretched between two optical traps. First, actin and myosin were brought close to each other while monitoring the process using epi-illumination. After binding of myosin to the actin filament, single turnovers of Cy3-ATP were observed after switching to TIRF excitation.

Just as actin filaments, long DNA molecules represent useful spacers that allow for the spatial separation of fluorescence excitation and bead trapping (Figure 6). Due to its length of ~16 μm, λ-DNA is an ideal spacer for combined OT-fluorescence measurements. But also other DNA molecules of micrometer length have been synthesized and used as spacers. DNA is easily attached to the trapping beads and a number of experiments have been performed to

Chemical Science Accepted Manuscript

investigate DNA-protein interactions. In the first experiment, the DNA was stretched between two optical traps while the force-dependent association and dissociation of single fluorescently labeled RNA polymerase molecules was monitored using TIRF excitation with a glass pedestal.[85] Other DNA binding proteins have been studied using widefield illumination. These include the recombinase RAD51,[86,87] human mitochondrial transcription factor A (TFAM)[88] and the bacterial DNA recombination protein RecA.[89] Further, the single strand binding proteins mtSSB (human mitochondrial single stranded binding protein) and RPA (replication protein A) have been used to monitor the appearance of single stranded DNA (ssDNA) when overstretching DNA.[90]

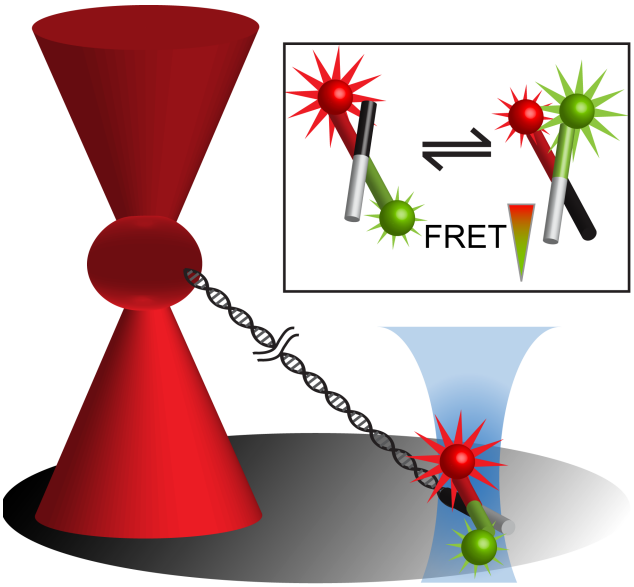

Figure 6. Long DNA spacers for simultaneous OT-FRET measurements. A FRET labeled biomolecule is tethered to a surface and connected to the optical trap *via* a long (λ-DNA) spacer. In this way the fluorescence detection (TIRF or confocal) is spatially separated from the high intensity trapping laser, circumventing enhanced photo bleaching and increased background fluorescence. Illustrated is the example of the Holliday Junction, as described by Hohng *et al*.[52]

Long λ-DNA spacers have also been used for studying the switching behavior of the Holliday junction as a function of force.[52] The Holliday junction exists in different conformations that can

Chemical Science Accepted Manuscript

be distinguished using FRET. Using a single trap configuration, the Holliday junction was immobilized on a cover slip and attached to the bead *via* a λ-DNA linker (Figure 6). A confocal microscope was used to monitor switching between the two conformations characterized by their different FRET efficiencies. The same experimental setup was used to investigate the mechanism of *E. coli* single strand binding (SSB) protein when moving on DNA. Using a FRET reporter system, it could be shown that SSB is sliding instead of rolling on ssDNA.[91]

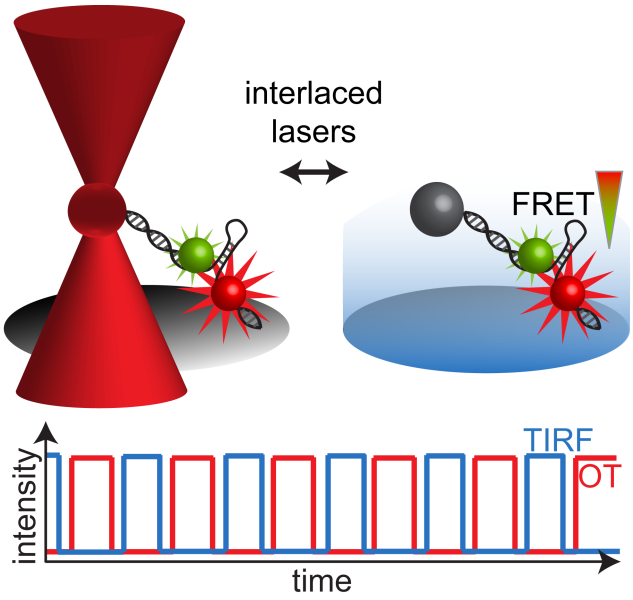

Figure 7. Interlaced OT and fluorescence excitation allowing for simultaneous OT and FRET measurements, without the need for long spacers. For sufficiently high switching frequencies (kHz) neither the trap performance, nor the fluorescence resolution (TIRF or confocal) is compromised. Illustrated is the example of a FRET labeled DNA hairpin, as described by Tarsa *et al*.[53]

The use of long spacers imposes strong constraints on the experimental design, limiting the biological systems that can be studied to molecular motors and processes involving nucleic acids. A more general strategy is the temporal separation of the trapping laser and the excitation laser. Using acousto-optical devices, trapping and fluorescence detection can be easily alternated. For sufficiently high modulation frequencies in the kHz range, neither the trap

Chemical Science Accepted Manuscript

stiffness nor the sensitivity of the fluorescence detection scheme is affected (Figure 7).[92] The first experiment using interlaced excitation was designed to study the force-induced rupture of a DNA duplex.[92] In this experiment Cy3 was used as fluorophore and its photostability was improved 20-fold. Subsequently, interlaced excitation enabled a detailed FRET study of a DNA hairpin (Figure 7). Several cycles of reversible opening and closing could be followed for 65 seconds.[53]

The above experiments have been performed using a single trap and TIRF excitation. In this configuration only two lasers need to be interlaced, whereas experiments with a dual trap require the synchronization of three laser lines. Different pulse schemes are possible involving sequential[93] or simultaneous illumination[94] of the two traps. Advanced dual-trap setups with interlaced trapping and fluorescence detection are technically challenging but clearly are the most powerful strategy developed so far to combine optical trapping with single molecule fluorescence detection.

Summarizing, OTs are perfectly compatible with either confocal or widefield fluorescence microscopy. Single trap configurations or pedestal shaped prisms also allow for TIRF excitation. Many strategies to overcome the enhanced photobleaching problem have been successfully developed and a number of biological systems have been measured with single molecule force and fluorescence resolution. Interlacing the trapping laser with the fluorescence excitation laser is the most general solution and has facilitated impressive single molecule fluorescence performance.

Combining magnetic tweezers with fluorescence detection

Combining magnetic tweezers with fluorescence microscopy offers additional possibilities for studying single molecule behavior. Force-clamp experiments can be easily combined with the application of torque and a number of molecules can be investigated in parallel. As force readout is achieved optically, the combination with fluorescence seems straightforward. The

Chemical Science Accepted Manuscript

beads can be illuminated with IR light so that the fluorescence signal can be separated from the bead images *via* dichroic mirrors. The MT performance should consequently not be affected by the presence of a fluorescence microscope. Integration with widefield techniques maintains the possibility for observing many molecules in parallel. Combinations with confocal microscopy eliminate this high throughput advantage and no description of a combined instrument has been reported so far.

Whereas force or torque detection is hardly affected in a combined setup, the fluorescence measurements suffer from background fluorescence originating from the magnetic beads. Most commercially available magnetic beads have a latex coating that is autofluorescent. Two exceptions are the irregularly shaped BioMagPlus beads (Polysciences) and ferromagnetic nanowires[42]. Both are only useful for a limited range of applications, however. BiomagPlus beads have been engineered for separation applications and, therefore, have a high magnetic content. Variations in their magnetic content lead to force differences of up to 100 % among different beads, restricting their use to experiments that require low accuracy. Ferromagnetic particles might show force fluctuations over time, as their magnetization is influenced by hysteresis. To overcome the problem of bead autofluorescence, a number of solutions have been found similar to the strategies employed in the AFM and OT setups.

The first setup based on an epifluorescence microscope was already established in 1992 by Smith & Bustamante.[95] A DNA molecule was bound with one end to the surface of a flow chamber and the free end was attached to a paramagnetic bead. When manipulating the bead with both magnetic and flow forces, it could be moved on a parabolic path. As the DNA was fluorescently labeled with a large number of ethidium bromide fluorophores, its movement could be followed. The analysis of the obtained force-extension curves yielded information about the elastic behavior of DNA and revealed that DNA elasticity is influenced by ethidium bromide intercalation.

Chemical Science Accepted Manuscript

A highly fluorescent reporter system was also employed for studying the enzyme DNA gyrase. Its activity was followed by tracking the angular displacement of a highly fluorescent rotor bead attached to the rotating DNA molecule[96] (Figure 8). The displacement of the bead is a direct measure of DNA supercoiling that results from gyrase activity. The MTs were needed to stretch the DNA molecule perpendicular to the surface. More importantly, gyrase activity could be studied as a function of the applied force. Besides using a highly fluorescent rotor bead, the experimental design included a 2.4 μm long DNA spacer to spatially separate the rotor bead from the magnetic bead avoiding fluorescence crosstalk.

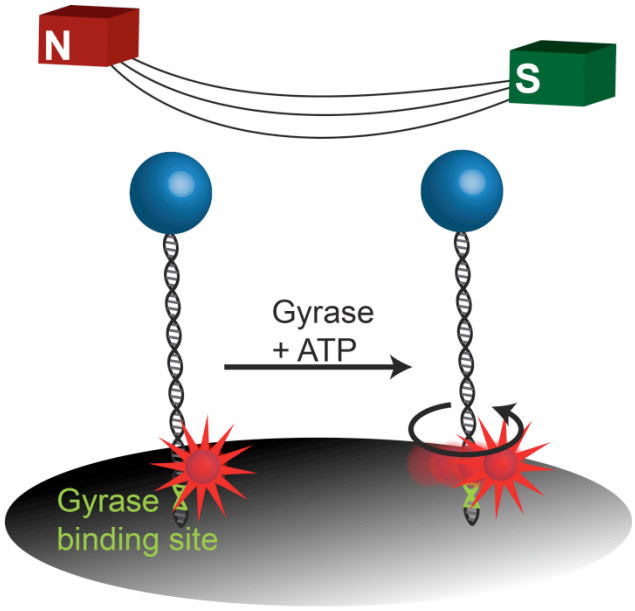

Figure 8. Brightfield-MT setup using a highly fluorescent rotor bead to track rotation of the DNA molecule caused by gyrase activity, as described by Gore *et al*.[96]

Even though the long DNA spacer improved the S:N ratio, single fluorophore detection is not possible in an epifluorescence microscope due to the large detection volume. This is especially critical in the presence of several fluorescing magnetic beads. TIRF microscopy has been used to overcome this problem. When using long spacers or analyzing a long molecule of interest, the small penetration depth of the evanescent field in the z-dimension allows for placing the fluorescing magnetic beads completely outside the fluorescence detection volume.[97–100] MTs

Chemical Science Accepted Manuscript

require surface tethered assays and the requirement to record fluorescence close to a surface does not add any further constraints. In order to use the space on top of the flow chamber for magnets, objective based TIRF is an evident choice.

This approach was first implemented by Shroff *et al*.[97] to characterize the stretching behavior of ssDNA in a combined force and fluorescence experiment (Figure 9). ssDNA oligonucleotides were labeled with two fluorophores forming a FRET pair and immobilized onto a cover slip. They were subsequently attached to the magnetic beads using a λ-DNA handle. As the DNA was stretched, the distance between the two fluorophores increased leading to a decrease in the FRET efficiency. As it was possible to detect the fluorescence of the individual chromophores, the force applied on the ssDNA could be directly related to the FRET efficiency.

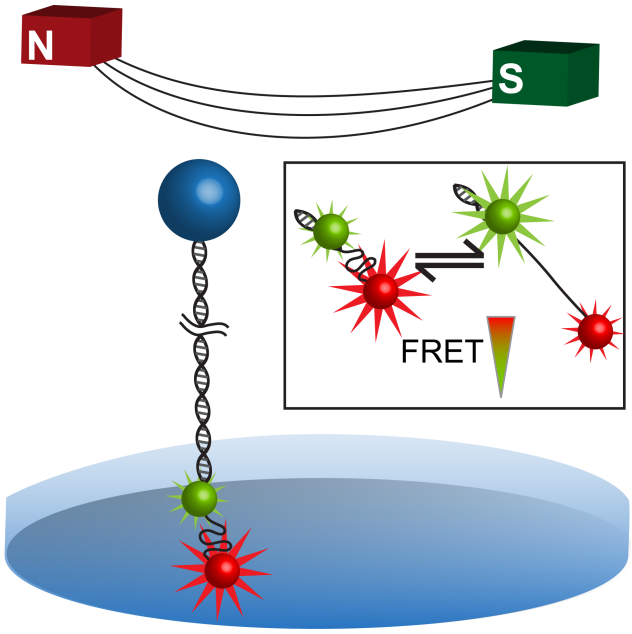

Figure 9. Long spacers for simultaneous MT and TIRF measurements. The long DNA spacer ensures that the fluorescent beads are located outside the evanescent field, significantly reducing the fluorescence background. Illustrated is a FRET-based DNA force sensor as described by Shroff *et al*.[97]

Chemical Science Accepted Manuscript

This experiment allowed the calibration of one of the first artificial molecular force sensors: the force applied on the molecule could be read out *via* fluorescence while the molecule was stretched. The dynamic range of this nanoscopic sensor is in the range of 0 - 20 pN and has subsequently been used for investigating the bending behavior of double stranded DNA (dsDNA) on small length scales.[101]

Using a similar experimental setup, the B-Z transition of DNA was studied as a function of tension and torsion applied to the DNA.[98] Z-DNA formation increases the length of the DNA molecule and can consequently be determined using FRET. In this experiment, a minimum force of 0.2 pN was applied to prevent coiling of the DNA that would pull the magnetic bead into the evanescent field causing background fluorescence. Lastly, a FRET reporter system was implemented to investigate the (un)folding pathways of G-quadruplex DNA when subjected to constant stretching forces ranging from 0.1 pN to 20 pN.[100]

TIRF excitation combined with a long DNA spacer was also used for studying the mechanism of the rotary motor responsible for packing DNA into bacteriophage Φ29.[99] A single fluorophore was coupled to the connector of the immobilized capsid. Using a prism-based TIRF setup that facilitated the detection of fluorescence polarization, it was shown that the connector is not rotating while the DNA is packed into the capsid. Clearly long spacers help to reduce the fluorescence background of the magnetic beads. Similar to the OT experiments, they are only useful for a small number of experimental designs, however, mostly involving nucleic acids.

An approach that tolerated or was not influenced by the autofluorescence of the magnetic beads was reported by Adachi *et al*.[102] who observed the conversion of Cy3-ATP by F_1-ATPase under forced rotation. While this TIRF experiment did not seem to suffer from the presence of the magnetic beads, other experiments have been designed that take advantage of the bead fluorescence or even use fluorescently labeled magnetic beads. Bead fluorescence allows for establishing the location of the magnetic beads. This strategy was successfully used for

Chemical Science Accepted Manuscript

investigating the mechanosensing properties of the protein talin.[7] Upon stretching, talin is expected to expose cryptic vinculin-binding sites. As the stretched talin molecules themselves were not fluorescently labeled, the autofluorescence of the magnetic beads allowed for their localization in the TIRF field of view. The vinculin molecules were labeled so that their binding to talin could be followed by fluorescence. The observed fluorescence signal at the position of a talin molecule was consequently the sum of the bead fluorescence and the fluorescence of the bound vinculin molecules. After the vinculin molecules were allowed to find exposed binding sites on talin, the sample was excited and the fluorescence signal was followed over time. The number of discrete photobleaching steps revealed the number of bound vinculin molecules and was found to vary as a function of the applied force.

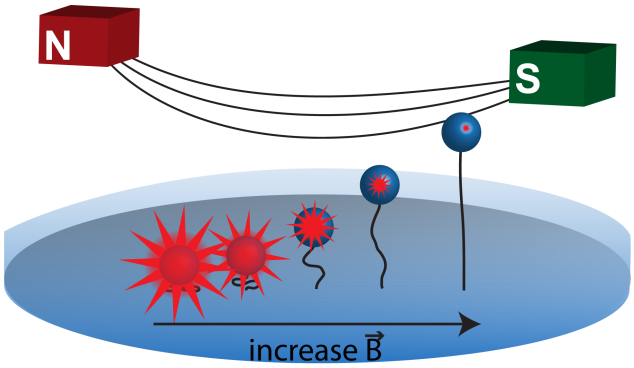

Figure 10. Height dependence of the fluorescence intensity in an evanescent field. The evanescent field decays exponentially from the surface. Consequently, also the fluorescence emission of a magnetic bead placed at different z-heights above the surface decays exponentially and can be employed for determining its position.[100,101]

The fluorescence of the magnetic beads cannot only be utilized to locate their position in the x-y plane. When using TIRF excitation, the bead fluorescence can be calibrated to determine the z-height of a fluorescent particle with sub-nanometer precision[103–105] (Figure 10). In a TIRF microscope the intensity of the evanescent field decreases exponentially as a function of z so that the fluorescence intensity is a direct measure of the distance between the bead and the

Chemical Science Accepted Manuscript

surface. Using electromagnetic tweezers,[104,106] the force can be easily altered throughout the experiment allowing for force-clamp measurements at different forces as well as force-ramp experiments. In one example the unfolding and refolding of Protein L was measured under force-clamp conditions in the low force regime, not easily accessible with AFM.[106] The fluorescence of the magnetic beads directly reported on the change in length resulting from unfolding or refolding of the protein. The (un)folding kinetics were determined from measurements at different forces. In force-ramp experiments, the bead fluorescence can be utilized to obtain the distance information required to construct force-distance curves.[104] Using DNA hybridization as a test case, a ssDNA molecule (200 bases long) was stretched in the presence and absence of a complementary DNA oligonucleotide (50 bases). As ssDNA and dsDNA possess different stiffness, the length of the double stranded fragment was obtained from fitting the force-distance curves with appropriate polymer models. The length of the double stranded section could be determined with the accuracy of one base pair. This result clearly proves that obtaining distance information from the bead fluorescence is more accurate than using the bead's interference fringes.

In summary, the above examples show that MTs are best combined with TIRF widefield microscopy. Although this combination is easily implemented, the autofluorescence of the magnetic beads currently limits the range of applications of this powerful approach. The development of non-fluorescent magnetic beads would circumvent the need for long spacers and facilitate a large number of novel applications for studying mechanosensitive proteins that cannot be coupled to DNA handles easily. Measurements that actually use the bead fluorescence for obtaining position information in 3 dimensions have not yet been combined with a fluorescent reporter system designed to report on molecular transitions. To achieve this goal, beads with a narrow fluorescence emission spectrum are needed so that the different fluorescence signals can be spectrally separated.

Chemical Science Accepted Manuscript

Limitations and future developments of combined force-fluorescence instruments

The above examples highlight the potential of combined force-fluorescence experiments for investigating force-structure-function relationships. A number of different setups have been implemented that facilitate the mechanical manipulation of a single molecule while providing either sequential (Figure 11a) or simultaneous (Figure 11b) fluorescence readout. These setups have now reached a high level of maturity. They have enabled many novel experiments where the effect of force on a variety of molecular systems has been studied, including protein and DNA folding, molecular interactions and catalytic reactions. Most importantly, the first natural molecular force sensors[7,13] and man-made molecular force probes have been characterized.[97,107]

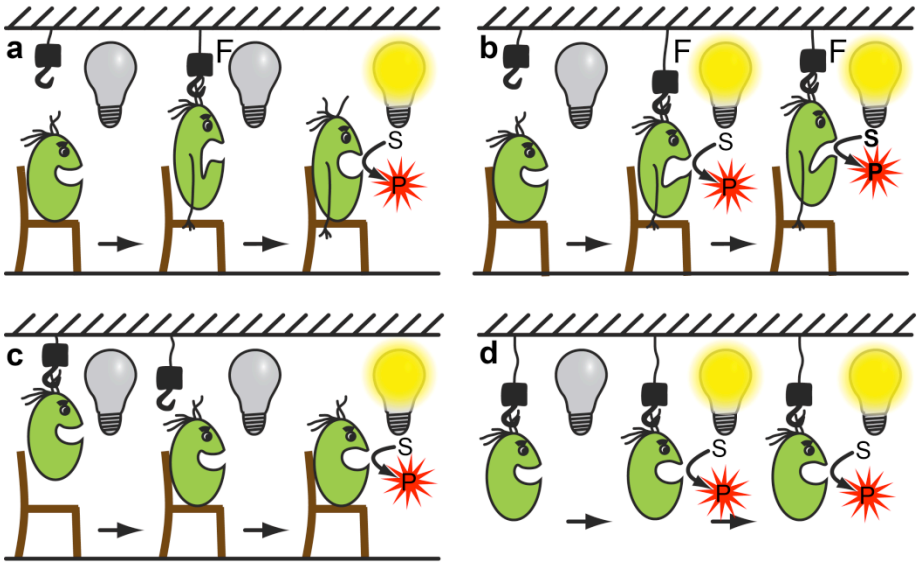

Figure 11. Summary of possible applications of combined force fluorescence instruments showing an enzymatic reaction as example. (a) sequential mechanical manipulation and fluorescence activity readout, (b) simultaneous mechanical manipulation and fluorescence measurement, (c) sequential positioning and fluorescence measurement, and (d) simultaneous positioning and fluorescence measurement.

Chemical Science Accepted Manuscript

Despite the enormous potential of combined setups, a few challenges remain. While the spatial resolution of the force-based techniques is in the low nanometer range, optical detection is diffraction limited. Depending on the surface density of the molecules under study, this mismatch in spatial resolution can cause the following problems: 1) The applied force might be used to switch on fluorescence, *e.g.* as the result of a catalytic reaction. In this case, the immobilized molecules do not need to carry a fluorescent label. Their surface density can be high, facilitating high interaction frequencies in the force spectroscopy experiment. Strategies need to be developed to ensure that the appearance of the fluorescence signal is indeed force induced. Unrelated events originating from one of the many neighboring molecules might randomly occur and be mistaken as a real force-induced event. 2) If all molecules on the surface are fluorescently labeled, their density needs to be low to ensure single molecule detection. In this case, the alignment of the force probe with the exact position of one molecule can become challenging. The use of point-spread functions may potentially overcome this problem in widefield microscopes using CCD detection. In confocal setups other solutions are needed that allow for positioning the molecule of interest in the optical detection volume. To achieve this goal, the positioning accuracy of force spectroscopy instruments can be utilized to transport and constrain a single molecule in the area optimized for fluorescence excitation (Figures 11c,d). The AFM allows for positioning the molecule in a certain area before the fluorescence measurement (Figure 11c). Using single molecule cut-and-paste,[66–68] even the positioning of individual molecules in zero mode waveguide structures has been demonstrated.[69] Dual-trap OTs operating in force-clamp mode can be used to move the molecule into the fluorescence detection volume during the measurement (Figure 11d).[91,93]

The combination of mechanical manipulation with fluorescence detection does not only rely on the site-specific application of the force at two defined positions, but might further require fluorescent labeling. The need for at least two defined coupling sites represents a challenge especially when studying proteins. Advanced protein engineering and bioconjugation strategies

Chemical Science Accepted Manuscript

need to be implemented that have to be adapted for every specific system under study. Introducing non-natural amino acids that facilitate the use of bioorthogonal reactions such as strain promoted alkyne-azide cycloaddition reactions[108] will only solve part of the problem. Protein samples do not normally contain a several micrometer long spacer such as λ-DNA. Instead protein-polymer conjugates or long engineered polyproteins[103,106] have to be designed. Even in the case of MT-fluorescence combinations, the throughput of such measurements remains small. This does not only restrict the number of molecules and modifications that can be studied, but, more importantly, limits the statistical accuracy when analyzing molecules that have been mechanically manipulated and their respective controls. Many other strategies are currently being developed that can eventually overcome these limitations and facilitate highly multiplexed measurements *in situ*.

Alternative Techniques Providing Mechanical Information

Force spectroscopy using the AFM, OTs or MTs is the gold standard for single molecule force measurements. These techniques allow the simultaneous application and measurement of the force with the same force probe at the single molecule level. They have two limitations in common: their throughput is low and they cannot be used *in situ*. Many alternative methods have been developed that address these limitations (table 1). These techniques are easier to implement but do not always provide single molecule resolution. Still, these techniques provide a very useful addition to the mechanical toolkit as they can also be used for the mechanical characterization of more complex systems, such as cells and materials.

Table 1. Alternative methods developed for studying mechanical processes.

Technique	Principle
Multifrequency	Multifrequency AFM is an imaging technique. Unlike with conventional

Chemical Science Accepted Manuscript

AFM[109]	tapping mode, which used only one frequency, several frequencies are recorded. The different frequencies give access to different modes. These can be imagined as different channels that give access to different sample properties, such as topography and mechanical information. In this way maps of local stiffness or viscoeleastic properties can be produced.
Traction force microscopy[110,111]	The forces exerted by cells growing on an elastic substrate lead to deformation of the substrate. This deformation is read out optically using microbeads or nanopillars. Fluorescent microbeads inside a thick elastic substrate film are tracked while a cell pull on the substrate. The force can be deduced from the bead displacement within a substrate of known elasticity. The films are usually made of polyacrylamide (PAA), which has the advantage of a tunable elasticity, and thus tunable sensitivity. Nanopillar substrates consist of elastomeric micropost arrays, *e.g.* made from polydimethylsiloxane (PDMS). The degree of micropost bending depends on the traction forces applied by the cell. The corresponding forces can be approximated by finite-element method (FEM) analysis. Traction force microscopy can only measure forces. The technique is not able to apply forces. It also does not provide single molecule resolution.
Ultrasound[19,24]	Acoustic pressure waves pass through a liquid and locally compress and expand it. The resulting cavitation bubbles implode leading to very high local strain rates. Ultrasound is frequently used in the Materials Science community in a technique called polymer mechanochemistry. The

Chemical Science Accepted Manuscript

	mechanosensitive molecule is inserted between two equally long polymers. Being pulled by the local strain, the polymers experience the mechanical force and transfer it to the molecule of interest. The strain rates and the corresponding molecular forces can be calculated for a given system.[26]
Flow-stretching[112–114]	Fluid flow can be used to exert forces on immobilized (bio)macromolecules such as DNA, provided that they are sufficiently large. The stretching force is increased when a micrometer-sized bead is attached to the free end of the molecule. The flow rate can be tuned to vary the shear rate and thus the shear stress acting on the molecule. Flow-stretching can be applied to single molecules. Knowledge of the local flow rate might allow a calibration of the force acting on the molecule.
Microfluidics[115]	Besides flow-stretching assays, microfuidic setups can be used in a number of different ways for exerting forces on molecules or cells. These include both continuous flow and droplet-based strategies where the liquid/droplet needs to squeeze through a small nozzle. Alternatively, a flexible membrane at a channel intersection can be used for stretching or compressing cells.[115] In some cases a quantification of the forces might be possible.
Rheology[116,117]	Rheology measures the deformation of a material (strain) as a response to an externally applied force (stress). Different geometries are possible allowing linear or rotational stress. The shear stress as well as the shear rate is well defined and tunable. In this way the elastic and viscous contributions to the bulk material properties are characterized. Rheology averages over a large number of molecules. A quantification of the

Chemical Science Accepted Manuscript

	molecular forces is not possible.

Many of the above techniques utilize an optical readout (traction force microscopy, flow-stretching and microfluidics) or can easily be combined with optical detection systems. Single molecule fluorescence detection has so far only been implemented in flow-stretching[112] and microfluidic assays.[118] In general, techniques that apply or measure forces near a surface (multifrequency AFM, traction force microscopy, flow-stretching assays) are most easily combined with wide field single molecule detection schemes. If the molecules are diffusing freely (ultrasound, microfluidics) or are distributed in a 3D matrix (traction force microscopy, rheology), confocal microscopy is the better choice. To illustrate the potential of combining these alternative techniques with fluorescence detection, one example of flow stretching and rheology are each described in the following.

In flow stretching, a long surface tethered (bio)polymer is stretched out in a fluid flow. Wide field detection is most frequently used as it allows for the observation of many molecules in parallel. The fluid flow aligns the molecules in the flow direction. Depending on the magnitude of the force, it might further partially or fully unfold the immobilized (bio)polymers. This technique has for example been used for studying the interaction of fluorescently labeled proteins with DNA.[112] In a different example, De Ceunynck et al.[113] studied the proteolytic cleavage of the blood plasma protein von Willebrand factor (vWF) using a fluorescence microscope combined with a flow cell. Single elongated strings of vWF were visualized using fluorescently labeled platelets that specifically bind to vWF molecules. Following the string length over time allows for the detection of vWF cleavage in the presence and absence of the protease ADAMTS13. Preceding cleavage, a local elongation of vWF was observed.

Rheology is normally used for bulk materials where many molecules are exposed to the stress at the same time. Also the strain response is determined as an average over many molecules.

Chemical Science Accepted Manuscript

The resulting stress-strain relationships provide information about the elastic and viscous properties of the material. The bulk properties are well defined, but the local forces remain unknown. Frequently studied samples are emulsions, gels or (bio)polymer networks. Combining rheology with single molecule fluorescence detection can potentially reveal heterogeneous stress distributions in these samples and provide valuable additional information about molecular processes. Rheology has already been integrated with confocal detection schemes. This does not only avoid surface effects, but also allows for scanning the sample in 3D. Even though confocal rheology setups are commercially available and are commonly used in the food industry,[116] the technique has only recently been implemented in biophysical and materials research. Using a confocal rheometer, Schmoller et al.[117] observed a fluorescently labeled, crosslinked actin network after exposing it to several rounds of stress. In between the deformation cycles 3D-image stacks were recorded with the confocal microscope. Comparing the images before and after applying the strain, rearrangements of the actin bundles were observed that resulted in a hardened network.[117]

Molecular Force Probes

The above examples show the power of these techniques, but also illustrate the difficulty of quantifying the molecular forces in these experiments. As the mechanical manipulation is often applied macroscopically, the molecular forces remain hidden and cannot always be easily quantified. Molecular force probes (MFPs) can potentially be integrated with these techniques and directly report on the molecular forces acting locally. MFPs respond to the applied force in a defined way and convert the mechanical signal into a different output signal, thereby replacing a macroscopic force probe such as an AFM cantilever. Fluorescence readout is the method of choice as optical microscopy is non-destructive and can be applied *in situ*. MFPs become an integral part of the system. They can also be inserted into cells, in the extracellular matrix or into synthetic polymeric materials allowing for *in situ* force measurements. Besides the unique

Chemical Science Accepted Manuscript

potential of being used *in situ*, MFPs have the additional advantage that they enable highly parallel measurements. As these force probes are single molecules, they are the smallest artificial sensors that can be designed. Smaller sensors are less sensitive to thermal fluctuations and consequently provide a higher sensitivity and force resolution.[64,119] As outlined in the introduction, force sensing molecules naturally exist in biological systems. These natural protein force sensors have very sophisticated structures and have evolved for a very specific function. It is consequently difficult to utilize them for measuring forces in a different context. Instead, a number of artificial force sensors with more simple designs have been developed.

Molecular force probes for biological systems

The first experimental proof that a molecule can replace a macroscopic force probe was shown in the so-called differential force assay. A differential force assay is most easily imagined as a molecular "tug-of-war" where a well-characterized molecular interaction competes against an interaction of unknown strength (Figure 12a). In such a test, the weaker interaction ruptures with a higher probability. Consequently, determining the rupture probability of the well-characterized interaction provided indirect information about the mechanical stability of the unknown interaction.[119–121] The possibility of comparing two molecular interactions directly, eliminated the need for a macroscopic force probe and allowed for parallel measurements. The power of the approach was demonstrated in an assay that compared a single nucleotide mismatch to the corresponding perfect match oligonucleotide. The two sequences could be clearly discriminated based on their rupture probabilities. This is not possible in an AFM measurement, demonstrating the superior sensitivity of the new assay. Such interaction-based sensors are highly useful. But using the sensor breaks the interaction, leading to its simultaneous disintegration.

Chemical Science Accepted Manuscript

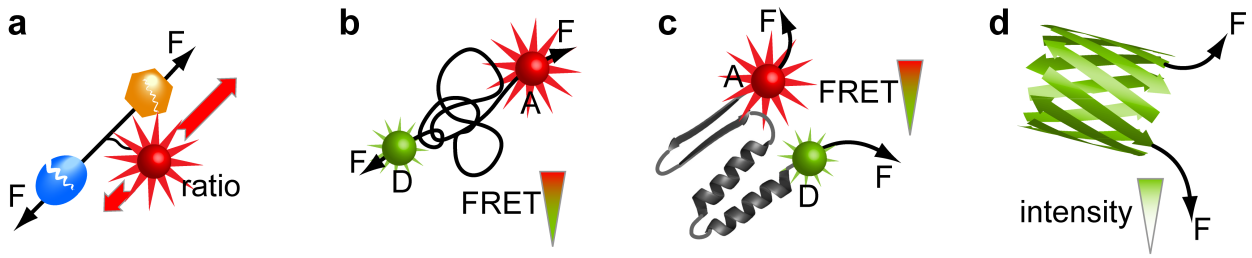

Figure 12. Designs of molecular force sensors. (a) An interaction-based sensor (blue) is placed in series with an unknown bond (orange). When pulling on the chain, the weaker bond will rupture with a higher probability. In a parallel test, the fluorescent label will remain with the stronger bond more frequently. (b) An entropic spring labeled with a FRET pair responds to a stretching force by a decrease in the FRET efficiency. (c) FRET-labeled structure-based sensors undergo a conformational change or unfold when exposed to a stretching force. The corresponding extension of the sensor is again detected as a change in its FRET efficiency. (d) The mechanical unfolding of a fluorescent protein leads to opening of its barrel-like structure accompanied by a decrease of its fluorescence intensity or a spectral change.

For many applications force sensors are needed that respond to the applied force in a reversible way and a number of new designs have been implemented. The first category utilizes polymers that act as entropic springs (Figure 12b), such as poly(ethylene glycol),[122] ssDNA[97] or the spider silk protein flagelliform.[107] Without an applied force, a flexible polymer adopts a random coil conformation. When pulled at its ends, the polymer is forced to leave this lowest energy conformation. The force required to stretch the polymer a certain distance, can be determined using known polymer models. The entropic springs mentioned above were labeled with a FRET pair on both ends. When stretching the polymer, the FRET efficiency was directly related to the separation distance and consequently to the force acting on the entropic spring. Entropic spring sensors operate in the low force range (up to 20 pN depending on the polymer used) and are therefore ideally suited for monitoring biologically relevant forces, *e.g.* generated by cells interacting with a surface.[122]

Chemical Science Accepted Manuscript

The second category follows the same principle as entropic springs, but contains a rather diverse set of structural motifs such as α-helices,[123] protein domains[124] or protein-protein interactions[125] (Figure 12c). When a force is applied on these structures, they will change their conformation leading to an increase in their end-to-end distance. These structure-based sensors are typically composed of polypeptides facilitating the generation of fusion proteins. In this way, fluorescent proteins can be used for the FRET readout enabling *in vivo* measurements that, for example, reported on the stretching of the extracellular matrix protein collagen-19 in living *C. elegans*.[126] The force range depends on the structure chosen and can be adapted to the expected force acting in the system under study. Unfortunately, the response of such a structure-based sensor cannot be modeled or predicted easily and no quantitative experiments have been done so far.

Lastly, the fluorescent molecule might be directly exposed to the force and change its fluorescence accordingly. For biological experiments, green fluorescent protein (GFP) and its derivatives are of special interest. GFP can be integrated into the protein and become exposed to the force acting on it (Figure 12d). The mechanical unfolding of GFP has been extensively studied with both AFM[127,128] and Molecular Dynamics simulations.[129] The forces required vary depending on the attachment position; loss of fluorescence is expected to occur once the first β-strand is removed from the β-barrel.[129] Although this appears to be a powerful and straightforward strategy, the experimental force range required to "switch off" GFP has not been directly determined in a combined force-fluorescence experiment and might be too high for biologically relevant measurements. More interestingly, it has been shown recently that a mechanical distortion of the β-barrel of a circularly permutated variant of yellow fluorescent protein (YFP) leads to a spectral shift of its absorption wavelength resulting from rearrangement of the amino acids forming the chromophore.[130] This approach seems more promising, but nothing is currently known about the forces required to achieve this effect.

Chemical Science Accepted Manuscript

Molecular force probes for materials applications

The field of mechanochemistry has evolved fast during the last years. Numerous examples demonstrate that mechanical force can "catalyze" thermodynamically slow chemical reactions such as the *cis-trans* isomerization of azobenzene,[22] the ring opening of cycloalkanes[33,131–135] and triazoles,[19] as well as the dissociation of metal-ligand coordination complexes.[136–139] More importantly, mechanical force can facilitate alternative high-barrier reaction pathways yielding thermally inaccessible products. This was impressively demonstrated for the mechanical ring-opening of *cis* and *trans* 1,2-dimethoxy benzocylcobutenes. While the thermally or photochemically activated reaction yielded different products starting from the *cis* or *trans* isomer, only a single product was obtained in the mechanically activated reaction.[132]

Besides fundamental studies aimed at investigating the molecular mechanisms of mechanophores, a number of mechanochemical reactions have been developed that yield an optically active or chemically reactive product. Covalently crosslinked within a polymeric material, these mechanophores have the potential to confer self-reporting or self-healing properties to the material. Ultimately, if the molecular forces required for activating the mechanophore are known, they can be used as MFPs. Of special interest are mechanophores that produce a fluorescent signal that can be read out in the visible range (Figure 13) just as for the biological force probes described above.

Several of the design principles used in biological systems can be directly applied in polymeric materials. It has been shown, for example, that FRET-labeled entropic spring sensors can report on the deformation of a bisurea-based thermoplastic elastomer consisting of hard bisurea and soft polytetrahydrofurane blocks.[140] In the non-deformed material, the flexible chains in the soft blocks closely adopted a random coil conformation. When mechanically deformed, the force elongated these polymer chains resulting in a change of the FRET efficiency. Further, the mechanical deformation of YFP has been used for detecting the failure of a glass-fiber

Chemical Science Accepted Manuscript

reinforced composite material.[141] Covalently crosslinked between the glass fibers and the surrounding epoxy resin, the YFP molecules performed as a sensitive reporter for fiber-matrix debonding. Presumably, the forces acting in this test system have been very high and caused the complete loss of YFP fluorescence.

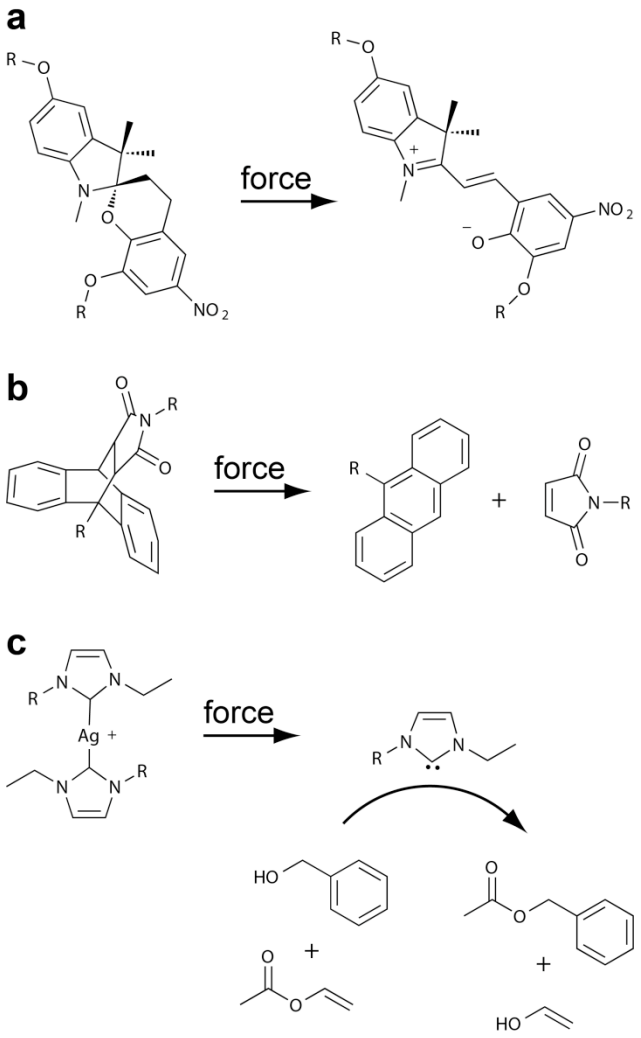

Figure 13. Examples of synthetic mechanophores. (a) Mechanofluorchromic dyes change their fluorescent properties as a function of the applied force. Shown is spiropyran that switches from a non-fluorescent structure to the highly fluorescent merocyanine.[23] (b) The mechanical rupture of a fluorogenic predetermined breaking point releases the fluorophore. Shown is an adduct of maleimide and the fluorophore anthracene.[20] (c) Mechanically activated silver-carbene

Chemical Science Accepted Manuscript

complexes can be utilized to catalyze a transesterification reaction.[24,147]

Gradual changes in the FRET ratio or a loss of fluorescence (turn-off probes) are useful readouts at high deformations where a large fraction of force probes show a response. In the early stages of the deformation process, however, only a small number of force probes react. As this will only result in a small change of the overall fluorescence signal, the onset of deformation is hard to follow. Here, turn-on probes are desired that produce a fluorescence signal once a certain threshold force is reached. The most well-known synthetic mechanophore with these properties is the mechanochromic dye spiropyran[23,142] (Figure 13a). Upon application of a force, the dye converts from the colorless spiropyran to the colored merocyanine form (λ_{abs} = 500 - 600 nm depending on the solvent[143]) that also emits fluorescence above 600 nm. Its applicability for investigating mechanical deformation has been shown in a number of different polymeric systems.[23,144–146] Even though Density Functional Theory (DFT) calculations have been performed[23,144] that support the proposed structural transition and the observed change in the absorption wavelength, no information is available about the minimum experimental force required for the structural change. Another drawback of the system is its low quantum yield in aqueous solvents,[143] limiting the application of this sensor to non-aqueous conditions.

An alternative fluorogenic MFP is based on a cycloaddition adduct of the fluorophore anthracene and maleimide[20] (Figure 13b). The cyclic adduct is non-fluorescent, but mechanical activation induces cycloreversion releasing the original anthracene dye. This has been demonstrated using a UV/VIS measurement after subjecting the polymer-functionalized adduct to ultrasound. Despite the low water solubility of anthracene this pre-determined mechanical breaking point is a promising candidate for biological applications, provided that low concentrations of the MFP are used.

In the above examples exactly one fluorescent molecule is produced as a result of the mechanochemical reaction. The sensitivity for observing the deformation process could

Chemical Science Accepted Manuscript

eventually be improved if every mechanochemical event would produce not only one but a large number of fluorophores. This signal amplification can be achieved when using a latent mechanocatalyst as the force probe.[24–26] The silver-carbene complex developed by Sijbesma and coworkers is of special interest in this context (Figure 13c). Upon rupture, a *N*-heterocyclic carbene is formed that catalyzes transesterification reactions.[24,147] It appears likely that the activated carbene is, for example, able to convert the fluorogenic substrate carboxyfluorescein diacetate to yield carboxyfluorescein as a detectable product.[148] Using a combined DFT - Molecular Dynamics approach, the force required to break the complex experimentally was predicted to be between 400 and 500 pN.[26] Unfortunately, the active species is not stable in the presence of water, again limiting its applicability.

Limitations and future developments of molecular force probes

The design and characterization of MFPs is an exciting new field. For biological applications, the MFPs are mostly biological molecules, whereas synthetic mechanophores are frequently used in polymeric materials. A few examples show that biomolecules can also be used as MFPs in synthetic materials and *vice versa*. The applicability of a MFP merely depends on the force range and the chemical environment of the probe as well as the strategies available to insert the probe into the system. In general one can assume that MFPs for biological systems need to be water soluble and respond in the low force range (< 100 pN) whereas non-aqueous environments and higher forces are typically required for materials applications.

Despite many impressive proof-of-principle experiments, the molecular forces required to obtain a response of the MFP have rarely been determined experimentally and theoretical predictions exist only for a very limited number of examples. This molecular knowledge is essential for the rational design of MFPs and for choosing the best probe for a certain application. Possible applications are just beginning to emerge. Some MFPs have already been used intracellularly or in the extracellular matrix.[107,126] MFPs are powerful tools that can further be combined with

Chemical Science Accepted Manuscript

techniques such as flow stretching, microfluidics and rheology. Current experiments mostly average over a large number of MFPs. A single molecule MFP readout will provide valuable information about the locally acting molecular forces thereby revealing the force distribution. Lastly, mechanically active molecules able to apply forces onto other molecules[101,149–151] will complement MFPs and provide new possibilities for studying mechanochemical effects at the molecular level in a growing number of applications.

Conclusions

The developments in single molecule methods and the development of molecular force probes can benefit from each other in a number of ways. The biggest weaknesses of the single molecule approach can be overcome with the use of molecular force probes that allow for parallel *in situ* measurements. Molecular force probes will also allow for the detection of molecular forces when bulk mechanical testing techniques are used. The missing calibration of molecular force probes can be directly addressed with single molecule experiments. Progress in all these areas requires a multidisciplinary approach that integrates the molecular designs with the newly developed combined force-fluorescence techniques. Despite common interests, little interaction is currently taking place between the Biophysics and Materials Science communities. The application of single molecule characterization methods to synthetic mechanophores and the design of new molecular force probes for both biological and materials applications are only two examples where collaboration can greatly advance our understanding of mechanical processes at the molecular level.

Chemical Science Accepted Manuscript

Acknowledgements

The authors thank Anna Wasiel and Stijn M. van Dongen for critically reading the manuscript. This work was supported by the Foundation for Fundamental Research on Matter (FOM) and

the Netherlands Organization for Scientific Research (NWO; VIDI grant and Gravitation program "Functional Molecular Systems").

References

1. H. Yu, J. K. Mouw, and V. M. Weaver, *Trends Cell Biol.*, 2011, **21**, 47–56.

2. A. J. Keung, S. Kumar, and D. V Schaffer, *Annu. Rev. Cell Dev. Biol.*, 2010, **26**, 533–556.

3. D. Gonzalez-Rodriguez, K. Guevorkian, S. Douezan, and F. Brochard-Wyart, *Science*, 2012, **338**, 910–917.

4. B. D. Hoffman and J. C. Crocker, *Annu. Rev. Biomed. Eng.*, 2009, **11**, 259–288.

5. P. A. Janmey and C. A. McCulloch, *Annu. Rev. Biomed. Eng.*, 2007, **9**, 1–34.

6. S. Sen and S. Kumar, *J. Biomech.*, 2010, **43**, 45–54.

7. A. del Rio, R. Perez-Jimenez, R. Liu, P. Roca-Cusachs, J. M. Fernandez, and M. P. Sheetz, *Science*, 2009, **323**, 638–641.

8. V. Vogel, *Annu. Rev. Biophys. Biomol. Struct.*, 2006, **35**, 459–488.

9. A. S. Adhikari, J. Chai, and A. R. Dunn, *J. Am. Chem. Soc.*, 2011, **133**, 1686–1689.

10. N. L. Stephenson and J. M. Avis, *Proc. Natl. Acad. Sci. USA*, 2012, **109**, E2757–E2765.

11. X. Zhang, K. Halvorsen, C.-Z. Zhang, W. P. Wong, and T. A. Springer, *Science*, 2009, **324**, 1330–1334.

12. E. M. Puchner, A. Alexandrovich, A. L. Kho, L. V Scha, B. Brandmeier, and F. Gra, *Proc. Natl. Acad. Sci. USA*, 2008, **105**, 13385–13390.

13. S. F. Heucke, E. M. Puchner, S. W. Stahl, A. W. Holleitner, H. E. Gaub, and P. Tinnefeld, *Int. J. Nanotechnol.*, 2013, **10**, 607–619.

14. B. T. Marshall, M. Long, J. W. Piper, T. Yago, R. P. McEver, and C. Zhu, *Nature*, 2003, **423**, 190–193.

15. O. Yakovenko, S. Sharma, M. Forero, V. Tchesnokova, P. Aprikian, B. Kidd, A. Mach, V. Vogel, E. Sokurenko, and W. E. Thomas, *J. Biol. Chem.*, 2008, **283**, 11596–11605.

16. M. D. Hager, P. Greil, C. Leyens, S. van der Zwaag, and U. S. Schubert, *Adv. Mater.*, 2010, **22**, 5424–5430.

Chemical Science Accepted Manuscript

17. Z. Huang and R. Boulatov, *Chem. Soc. Rev.*, 2011, **40**, 2359–2384.

18. K. Ariga, T. Mori, and J. P. Hill, *Adv. Mater.*, 2012, **24**, 158–176.

19. J. N. Brantley, K. M. Wiggins, and C. W. Bielawski, *Science*, 2011, **333**, 1606–1609.

20. K. M. Wiggins, J. A. Syrett, D. M. Haddleton, and C. W. Bielawski, *J. Am. Chem. Soc.*, 2011, **133**, 7180–7189.

21. Y. Chen, a J. H. Spiering, S. Karthikeyan, G. W. M. Peters, E. W. Meijer, and R. P. Sijbesma, *Nat. Chem.*, 2012, **4**, 559–562.

22. T. Hugel, N. B. Holland, A. Cattani, L. Moroder, M. Seitz, and H. E. Gaub, *Science*, 2002, **296**, 1103–1106.

23. D. A. Davis, A. Hamilton, J. Yang, L. D. Cremar, D. Van Gough, S. L. Potisek, M. T. Ong, P. V Braun, T. J. Martínez, S. R. White, J. S. Moore, and N. R. Sottos, *Nature*, 2009, **459**, 68–72.

24. A. Piermattei, S. Karthikeyan, and R. P. Sijbesma, *Nat. Chem.*, 2009, **1**, 133–137.

25. A. G. Tennyson, K. M. Wiggins, and C. W. Bielawski, *J. Am. Chem. Soc.*, 2010, **132**, 16631–16636.

26. R. Groote, B. M. Szyja, E. A. Pidko, E. J. M. Hensen, and R. P. Sijbesma, *Macromolecules*, 2011, **44**, 9187–9195.

27. K. M. Wiggins, J. N. Brantley, and C. W. Bielawski, *Chem. Soc. Rev.*, 2013, **42**, 7130–7147.

28. C. Bustamante, Y. R. Chemla, N. R. Forde, and D. Izhaky, *Annu. Rev. Biochem.*, 2004, **73**, 705–748.

29. E. Evans and K. Ritchie, *Biophys. J.*, 1997, **72**, 1541–1555.

30. E. Evans, *Annu. Rev. Biophys. Biomol. Struct.*, 2001, **30**, 105–128.

31. O. K. Dudko, G. Hummer, and A. Szabo, *Proc. Natl. Acad. Sci. USA*, 2008, **105**, 15755–15760.

32. M. Schlierf and M. Rief, *Biophys. J.*, 2006, **90**, L33–L35.

33. H. M. Klukovich, T. B. Kouznetsova, Z. S. Kean, J. M. Lenhardt, and S. L. Craig, *Nat. Chem.*, 2013, **5**, 110–114.

34. P. Hinterdorfer and Y. F. Dufrêne, *Nat. Methods*, 2006, **3**, 347–355.

35. I. De Vlaminck and C. Dekker, *Annu. Rev. Biophys.*, 2012, **41**, 453–472.

Chemical Science Accepted Manuscript

36. K. C. Neuman and A. Nagy, *Nat. Methods*, 2008, **5**, 491–505.

37. J. R. Moffitt, Y. R. Chemla, S. B. Smith, and C. Bustamante, *Annu. Rev. Biochem.*, 2008, **77**, 205–228.

38. E. M. Puchner and H. E. Gaub, *Curr. Opin. Struct. Biol.*, 2009, **19**, 605–614.

39. A. Engel and D. J. Müller, *Nat. Struct. Biol.*, 2000, **7**, 715–718.

40. A. Ashkin, J. M. Dziedzic, J. E. Bjorkholm, and S. Chu, *Opt. Lett.*, 1986, **11**, 288–290.

41. J. W. Shaevitz, E. A. Abbondanzieri, R. Landick, and S. M. Block, *Nature*, 2003, **426**, 684–687.

42. M. Tanase, N. Biais, and M. Sheetz, *Methods Cell Biol.*, 2007, **83**, 473–493.

43. M. E. J. Friese, T. A. Nieminen, N. R. Heckenberg, and H. Rubinsztein-Dunlop, *Nature*, 1998, **395**, 348–350.

44. A. Yildiz and P. R. Selvin, *Acc. Chem. Res.*, 2005, **38**, 574–582.

45. T. A. Klar, S. Jakobs, M. Dyba, A. Egner, and S. W. Hell, *Proc. Natl. Acad. Sci. USA*, 2000, **97**, 8206–8210.

46. T. Dertinger, R. Colyer, G. Iyer, S. Weiss, and J. Enderlein, *Proc. Natl. Acad. Sci. USA*, 2009, **106**, 22287–22292.

47. S. T. Hess, T. P. K. Girirajan, and M. D. Mason, *Biophys. J.*, 2006, **91**, 4258–4272.

48. M. J. Rust, M. Bates, and X. Zhuang, *Nat. Methods*, 2006, **3**, 793–795.

49. G. Patterson, M. Davidson, S. Manley, and J. Lippincott-Schwartz, *Annu. Rev. Phys. Chem.*, 2010, **61**, 345–367.

50. K. Blank, G. De Cremer, and J. Hofkens, *Biotechnol. J.*, 2009, **4**, 465–479.

51. V. I. Claessen, H. Engelkamp, P. C. M. Christianen, J. C. Maan, R. J. M. Nolte, K. Blank, and A. E. Rowan, *Annu. Rev. Anal. Chem.*, 2010, **3**, 319–340.

52. S. Hohng, R. Zhou, M. K. Nahas, J. Yu, K. Schulten, D. M. J. Lilley, and T. Ha, *Science*, 2007, **318**, 279–283.

53. P. B. Tarsa, R. R. Brau, M. Barch, J. M. Ferrer, Y. Freyzon, P. Matsudaira, and M. J. Lang, *Angew. Chem. Int. Ed.*, 2007, **46**, 1999–2001.

54. T. Ha, A. Y. Ting, J. Liang, W. B. Caldwell, A. A. Deniz, D. S. Chemla, P. G. Schultz, and S. Weiss, *Proc. Natl. Acad. Sci. USA*, 1999, **96**, 893–898.

55. T. Förster, *Annalen der Physik*, 1948, **437**, 55–75.

Chemical Science Accepted Manuscript

56. D. L. Dexter, *J. Chem. Phys.*, 1953, **21**, 836–850.

57. P. Tinnefeld and M. Sauer, *Angew. Chem. Int. Ed.*, 2005, **44**, 2642–2671.

58. R. Roy, S. Hohng, and T. Ha, *Nat. Methods*, 2008, **5**, 507–516.

59. J. Hohlbein, K. Gryte, M. Heilemann, and A. N. Kapanidis, *Phys. Biol.*, 2010, **7**, 1–22.

60. R. J. Owen, C. D. Heyes, and G. U. Nienhaus, *Biopolymers*, 2005, **82**, 410–414.

61. H. Gumpp, S. W. Stahl, M. Strackharn, E. M. Puchner, and H. E. Gaub, *Rev. Sci. Instrum.*, 2009, **80**, 063704.

62. A. Gaiduk, R. Kühnemuth, M. Antonik, and C. A. M. Seidel, *ChemPhysChem*, 2005, **6**, 976–983.

63. A. Toda, M. Kitazawa, and A. Yagi, *Jpn. J. Appl. Phys.*, 2004, **43**, 4671–4675.

64. M. B. Viani, T. E. Schaffer, M. Rief, H. E. Gaub, and P. K. Hansma, *J. Appl. Phys.*, 1999, **86**, 2258–2262.

65. T. Cordes, M. Strackharn, S. W. Stahl, W. Summerer, C. Steinhauer, C. Forthmann, E. M. Puchner, J. Vogelsang, H. E. Gaub, and P. Tinnefeld, *Nano Lett.*, 2010, **10**, 645–651.

66. S. K. Kufer, E. M. Puchner, H. Gumpp, T. Liedl, and H. E. Gaub, *Science*, 2008, **319**, 594–596.

67. E. M. Puchner, S. K. Kufer, M. Strackharn, S. W. Stahl, and H. E. Gaub, *Nano Lett.*, 2008, **8**, 3692–3695.

68. S. K. Kufer, M. Strackharn, S. W. Stahl, H. Gumpp, E. M. Puchner, and H. E. Gaub, *Nat. Nanotechnol.*, 2009, **4**, 45–49.

69. S. F. Heucke, F. Baumann, G. P. Acuna, P. M. D. Severin, S. W. Stahl, M. Strackharn, I. H. Stein, P. Altpeter, P. Tinnefeld, and H. E. Gaub, *Nano Lett.*, 2013.

70. A. Hards, C. Zhou, M. Seitz, C. Bräuchle, and A. Zumbusch, *ChemPhysChem*, 2005, **6**, 534–540.

71. S. Felekyan, M. Antonik, A. Gaiduk, R. Ku, W. Becker, V. Kudryavtsev, C. Sandhagen, and C. A. M. Seidel, *Microsc. Res. Tech.*, 2007, **70**, 433–441.

72. M. S. Z. Kellermayer, A. Karsai, A. Kengyel, A. Nagy, P. Bianco, T. Huber, A. Kulcsár, C. Niedetzky, R. Proksch, and L. Grama, *Biophys. J.*, 2006, **91**, 2665–2677.

73. H. Gumpp, E. M. Puchner, J. L. Zimmermann, U. Gerland, H. E. Gaub, and K. Blank, *Nano Lett.*, 2009, **9**, 3290–3295.

74. Y. He, M. Lu, J. Cao, and H. P. Lu, *ACS Nano*, 2012, **6**, 1221–1229.

Chemical Science Accepted Manuscript

75. M. A. Van Dijk, L. C. Kapitein, J. Van Mameren, C. F. Schmidt, and E. J. G. Peterman, *J. Phys. Chem. B*, 2004, **108**, 6479–6484.

76. J. M. Ferrer, D. Fangyuan, R. R. Brau, P. B. Tarsa, and M. J. Lang, *Curr. Pharm. Biotechnol.*, 2009, **10**, 502–507.

77. M. J. Lang, P. M. Fordyce, and S. M. Block, *J. Biol.*, 2003, **2**, 6.1–6.4.

78. A. Ishijima, H. Kojima, T. Funatsu, M. Tokunaga, H. Higuchi, H. Tanaka, and T. Yanagida, *Cell*, 1998, **92**, 161–171.

79. S. Chu, *Science*, 1991, **253**, 861–866.

80. M. L. Bennink, O. D. Schärer, R. Kanaar, K. Sakata-Sogawa, J. M. Schins, J. S. Kanger, B. G. de Grooth, and J. Greve, *Cytometry*, 1999, **36**, 200–208.

81. A. Biebricher, W. Wende, C. Escudé, A. Pingoud, and P. Desbiolles, *Biophys. J.*, 2009, **96**, L50–L52.

82. M. Capitanio, D. Maggi, F. Vanzi, and F. S. Pavone, *J. Opt. A: Pure Appl. Opt.*, 2007, **9**, S157–S163.

83. U. Resch-Genger, M. Grabolle, S. Cavaliere-Jaricot, R. Nitschke, and T. Nann, *Nat. Methods*, 2008, **5**, 763–775.

84. K. Saito, T. Aoki, and T. Yanagida, *Biophys. J.*, 1994, **66**, 769–777.

85. Y. Harada, T. Funatsu, K. Murakami, Y. Nonoyama, A. Ishihama, and T. Yanagida, *Biophys. J.*, 1999, **76**, 709–715.

86. J. Van Mameren, M. Modesti, R. Kanaar, C. Wyman, G. J. L. Wuite, and E. J. G. Peterman, *Biophys. J.*, 2006, **91**, L78–L80.

87. J. Van Mameren, M. Modesti, R. Kanaar, C. Wyman, E. J. G. Peterman, and G. J. L. Wuite, *Nature*, 2009, **457**, 745–748.

88. G. Farge, N. Laurens, O. D. Broekmans, S. M. J. L. van den Wildenberg, L. C. M. Dekker, M. Gaspari, C. M. Gustafsson, E. J. G. Peterman, M. Falkenberg, and G. J. L. Wuite, *Nat. Commun.*, 2012, **3**, 1–9.

89. A. L. Forget, C. C. Dombrowski, I. Amitani, and S. C. Kowalczykowski, *Nat. Protoc.*, 2013, **8**, 525–538.

90. J. Van Mameren, P. Gross, G. Farge, P. Hooijman, M. Modesti, M. Falkenberg, G. J. L. Wuite, and E. J. G. Peterman, *Proc. Natl. Acad. Sci. USA*, 2009, **106**, 18231–18236.

91. R. Zhou, A. G. Kozlov, R. Roy, J. Zhang, S. Korolev, and T. M. Lohman, *Cell*, 2011, **146**, 222–232.

Chemical Science Accepted Manuscript

92. R. R. Brau, P. B. Tarsa, J. M. Ferrer, P. Lee, and M. J. Lang, *Biophys. J.*, 2006, **91**, 1069–1077.

93. M. J. Comstock, T. Ha, and Y. R. Chemla, *Nat. Methods*, 2011, **8**, 335–340.

94. G. Sirinakis, Y. Ren, Y. Gao, Z. Xi, and Y. Zhang, *Rev. Sci. Instrum.*, 2012, **83**, 1–9.

95. S. B. Smith, L. Finzi, and C. Bustamante, *Science*, 1992, **258**, 1122–1126.

96. J. Gore, Z. Bryant, M. D. Stone, M. Nöllmann, N. R. Cozzarelli, and C. Bustamante, *Nature*, 2006, **439**, 100–104.

97. H. Shroff, B. M. Reinhard, M. Siu, H. Agarwal, A. Spakowitz, and J. Liphardt, *Nano Lett.*, 2005, **5**, 1509–1514.

98. M. Lee, S. H. Kim, and S.-C. Hong, *Proc. Natl. Acad. Sci. USA*, 2010, **107**, 4985–4990.

99. T. Hugel, J. Michaelis, C. L. Hetherington, P. J. Jardine, S. Grimes, J. M. Walter, W. Falk, D. L. Anderson, and C. Bustamante, *PLoS Biol.*, 2007, **5**, 0558–0567.

100. X. Long, J. W. Parks, C. R. Bagshaw, and M. D. Stone, *Nucleic Acids Res.*, 2013, **41**, 2746–2755.

101. H. Shroff, D. Sivak, J. J. Siegel, A. L. McEvoy, M. Siu, A. Spakowitz, P. L. Geissler, and J. Liphardt, *Biophys. J.*, 2008, **94**, 2179–2186.

102. K. Adachi, K. Oiwa, T. Nishizaka, S. Furuike, H. Noji, H. Itoh, M. Yoshida, and K. Kinosita, *Cell*, 2007, **130**, 309–321.

103. A. Sarkar, R. B. Robertson, and J. M. Fernandez, *Proc. Natl. Acad. Sci. USA*, 2004, **101**, 12882–12886.

104. P. M. Oliver, J. S. Park, and D. Vezenov, *Nanoscale*, 2011, **3**, 581–591.

105. A. Bijamov, F. Shubitidze, P. M. Oliver, and D. V Vezenov, *Langmuir*, 2010, **26**, 12003–12011.

106. R. Liu, S. Garcia-Manyes, A. Sarkar, C. L. Badilla, and J. M. Fernández, *Biophys. J.*, 2009, **96**, 3810–3821.

107. C. Grashoff, B. D. Hoffman, M. D. Brenner, R. Zhou, M. Parsons, M. T. Yang, M. A. McLean, S. G. Sligar, C. S. Chen, T. Ha, and M. A. Schwartz, *Nature*, 2010, **466**, 263–266.

108. M. F. Debets, S. S. van Berkel, J. Dommerholt, A. T. J. Dirks, F. P. J. T. Rutjes, and F. L. van Delft, *Acc. Chem. Res.*, 2011, **44**, 805–815.

109. R. Garcia and E. T. Herruzo, *Nat. Nanotechnol.*, 2012, **7**, 217–226.

Chemical Science Accepted Manuscript

110. B. Sabass, M. L. Gardel, C. M. Waterman, and U. S. Schwarz, *Biophys. J.*, 2008, **94**, 207–220.

111. J. Fu, Y.-K. Wang, M. T. Yang, R. A. Desai, X. Yu, Z. Liu, and C. S. Chen, *Nat. Methods*, 2010, **7**, 733–736.

112. J. S. Leith, A. Tafvizi, F. Huang, W. E. Uspal, P. S. Doyle, A. R. Fersht, L. A. Mirny, and A. M. van Oijen, *Proc. Natl. Acad. Sci. USA*, 2012, **109**, 16552–16557.

113. K. De Ceunynck, S. Rocha, H. B. Feys, S. F. De Meyer, H. Uji-i, H. Deckmyn, J. Hofkens, and K. Vanhoorelbeke, *J. Biol. Chem.*, 2011, **286**, 36361–36367.

114. J. Jing, J. Reed, J. Huang, X. Hu, V. Clarke, J. Edington, D. Housman, T. S. Anantharaman, E. J. Huff, B. Mishra, B. Porter, A. Shenker, E. Wolfson, C. Hiort, R. Kantor, C. Aston, and D. C. Schwartz, *Proc. Natl. Acad. Sci. USA*, 1998, **95**, 8046–8051.

115. F. Kurth, K. Eyer, A. Franco-Obregón, and P. S. Dittrich, *Curr. Opin. Chem. Biol.*, 2012, **16**, 400–408.

116. E. van der Linden, L. Sagis, and P. Venema, *Curr. Opin. Colloid Interface Sci.*, 2003, **8**, 349–358.

117. K. M. Schmoller, P. Fernández, R. C. Arevalo, D. L. Blair, and A. R. Bausch, *Nat. Commun.*, 2010, **1**, 134.

118. P. S. Dittrich and A. Manz, *Anal. Bioanal. Chem.*, 2005, **382**, 1771–1782.

119. C. Albrecht, K. Blank, M. Lalic-Mülthaler, S. Hirler, T. Mai, I. Gilbert, S. Schiffmann, T. Bayer, H. Clausen-Schaumann, and H. E. Gaub, *Science*, 2003, **301**, 367–370.

120. K. Blank, T. Mai, I. Gilbert, S. Schiffmann, J. Rankl, R. Zivin, C. Tackney, T. Nicolaus, K. Spinnler, F. Oesterhelt, M. Benoit, H. Clausen-Schaumann, and H. E. Gaub, *Proc. Natl. Acad. Sci. USA*, 2003, **100**, 11356–11360.

121. G. Neuert, C. H. Albrecht, and H. E. Gaub, *Biophys. J.*, 2007, **93**, 1215–1223.

122. D. R. Stabley, C. Jurchenko, S. S. Marshall, and K. S. Salaita, *Nat. Methods*, 2012, **9**, 64–67.

123. F. Meng, T. M. Suchyna, and F. Sachs, *FEBS J.*, 2008, **275**, 3072–3087.

124. F. Meng and F. Sachs, *J. Cell Sci.*, 2011, **124**, 261–269.

125. S. Iwai and T. Q. P. Uyeda, *Proc. Natl. Acad. Sci. USA*, 2008, **105**, 16882–16887.

126. F. Meng, T. M. Suchyna, E. Lazakovitch, R. M. Gronostajski, and F. Sachs, *Cell. Mol. Bioeng.*, 2011, **4**, 148–159.

127. H. Dietz and M. Rief, *Proc. Natl. Acad. Sci. USA*, 2004, **101**, 16192–16197.

Chemical Science Accepted Manuscript

128. H. Dietz and M. Rief, *Proc. Natl. Acad. Sci. USA*, 2006, **103**, 1244–1247.

129. J. Saeger, V. P. Hytönen, E. Klotzsch, and V. Vogel, *PLoS One*, 2012, **7**, e46962.

130. T. Ichimura, H. Fujita, K. Yoshizawa, and T. M. Watanabe, *Chem. Commun.*, 2012, **48**, 7871–7873.

131. J. M. Lenhardt, J. W. Ogle, M. T. Ong, R. Choe, T. J. Martinez, and S. L. Craig, *J. Am. Chem. Soc.*, 2011, **133**, 3222–5.

132. C. R. Hickenboth, J. S. Moore, S. R. White, N. R. Sottos, J. Baudry, and S. R. Wilson, *Nature*, 2007, **446**, 423–427.

133. H. M. Klukovich, Z. S. Kean, S. T. Iacono, and S. L. Craig, *J. Am. Chem. Soc.*, 2011, **133**, 17882–17888.

134. M. J. Kryger, A. M. Munaretto, and J. S. Moore, *J. Am. Chem. Soc.*, 2011, **133**, 18992–18998.

135. Z. S. Kean, A. L. Black Ramirez, Y. Yan, and S. L. Craig, *J. Am. Chem. Soc.*, 2012, **134**, 12939–12942.

136. M. Conti, G. Falini, and B. Samorì, *Angew. Chem. Int. Ed.*, 2000, **39**, 215–218.

137. M. Kudera, C. Eschbaumer, H. E. Gaub, and U. S. Schubert, *Adv. Funct. Mater.*, 2003, **13**, 615–620.

138. C. Verbelen, H. J. Gruber, and Y. F. Dufre, *J. Mol. Recognit.*, 2007, **20**, 490–494.

139. S. Karthikeyan, S. L. Potisek, A. Piermattei, and R. P. Sijbesma, *J. Am. Chem. Soc.*, 2008, **130**, 14968–14969.

140. S. Karthikeyan and R. P. Sijbesma, *Macromolecules*, 2009, **42**, 5175–5178.

141. K. Makyła, C. Müller, S. Lörcher, T. Winkler, M. G. Nussbaumer, M. Eder, and N. Bruns, *Adv. Mater.*, 2013, **25**, 2701–2706.

142. S. L. Potisek, D. A. Davis, N. R. Sottos, S. R. White, and J. S. Moore, *J. Am. Chem. Soc.*, 2007, **129**, 13808–13809.

143. M.-Q. Zhu, L. Zhu, J. J. Han, W. Wu, J. K. Hurst, and A. D. Q. Li, *J. Am. Chem. Soc.*, 2006, **128**, 4303–4309.

144. G. O'Bryan, B. M. Wong, and J. R. McElhanon, *ACS Appl. Mater. Interfaces*, 2010, **2**, 1594–1600.

145. B. A. Beiermann, S. L. B. Kramer, J. S. Moore, S. R. White, and N. R. Sottos, *ACS Macro Lett.*, 2012, **1**, 163–166.

Chemical Science Accepted Manuscript

146. C. K. Lee, B. A. Beiermann, M. N. Silberstein, J. Wang, J. S. Moore, N. R. Sottos, and P. V. Braun, *Macromolecules*, 2013, **46**, 3746–3752.

147. R. Groote, L. van Haandel, and R. P. Sijbesma, *J. Polym. Sci., Part A: Polym. Chem.*, 2012, **50**, 4929–4935.

148. M. B. J. Roeffaers, B. F. Sels, H. Uji-I, F. C. De Schryver, P. A. Jacobs, D. E. De Vos, and J. Hofkens, *Nature*, 2006, **439**, 572–575.

149. G. Zocchi, *Annu. Rev. Biophys.*, 2009, **38**, 75–88.

150. M. V Golynskiy, M. S. Koay, J. L. Vinkenborg, and M. Merkx, *ChemBioChem*, 2011, **12**, 353–361.

151. Q. Yang, Z. Huang, T. J. Kucharski, D. Khvostichenko, J. Chen, and R. Boulatov, *Nat. Nanotechnol.*, 2009, **4**, 302–306.

Chemical Science Accepted Manuscript